Geomorphology xxx (2015) xxx–xxx

Contents lists available at ScienceDirect

Geomorphology

journal homepage: www.elsevier.com/locate/geomorph

Review

New insights into the mechanics of fluvial bedrock erosion through flume experiments and theory

Michael P. Lamb [a,*], Noah J. Finnegan [b], Joel S. Scheingross [a], Leonard S. Sklar [c]

[a] Division of Geological and Planetary Sciences, California Institute of Technology, Pasadena, CA, USA
[b] Department of Earth and Planetary Sciences, University of California, Santa Cruz, CA, USA
[c] Department of Earth & Climate Sciences, San Francisco State University, San Francisco, CA, USA

ARTICLE INFO

Article history:
Received 24 May 2014
Received in revised form 26 February 2015
Accepted 2 March 2015
Available online xxxx

Keywords:
River incision
Bedrock erosion
Fluvial geomorphology
Abrasion
Plucking
Flume experiments

ABSTRACT

River incision into bedrock drives the topographic evolution of mountainous terrain and may link climate, tectonics, and topography over geologic time scales. Despite its importance, the mechanics of bedrock erosion are not well understood because channel form, river hydraulics, sediment transport, and erosion mechanics coevolve over relatively long time scales that prevent direct observations, and because erosive events occur intermittently and are difficult and dangerous to measure. Herein we synthesize how flume experiments using erodible bedrock simulants are filling these knowledge gaps by effectively accelerating the pace of landscape evolution under reduced scale in the laboratory. We also build on this work by providing new theory for rock resistance to abrasion, thresholds for plucking by vertical entrainment, sliding and toppling, and by assessing bedrock-analog materials. Bedrock erosion experiments in the last 15 years reveal that the efficiency of rock abrasion scales inversely with the square of rock tensile strength, sediment supply has a dominant control over bed roughness and abrasion rates, suspended sediment is an efficient agent of erosion, and feedbacks with channel form and roughness strongly influence erosion rates. Erodibility comparisons across rock, concrete, ice, and foam indicate that, for a given tensile strength, abrasion rates are insensitive to elasticity. The few experiments that have been conducted on erosion by plucking highlight the importance of block protrusion height above the river bed, and the dominance of block sliding and toppling at knickpoints. These observations are consistent with new theory for the threshold Shields stress to initiate plucking, which also suggests that erosion rates in sliding- and toppling-dominated rivers are likely transport limited. Major knowledge gaps remain in the processes of erosion via plucking of bedrock blocks where joints are not river-bed parallel; waterfall erosion by toppling and plunge-pool erosion; feedbacks between weathering and physical erosion; erosional bedforms; and morphodynamic feedbacks between channel form and erosion rates. Despite scaling challenges, flume experiments continue to provide much needed tests of existing bedrock-erosion theory, force development of new theory, and yield insight into the mechanics of landscapes.

Contents

* Corresponding author. Tel.: +1 626 395 3612.
E-mail address: mpl@gps.caltech.edu (M.P. Lamb).

http://dx.doi.org/10.1016/j.geomorph.2015.03.003
0169-555X/

1. Introduction

Models of landscape evolution driven by fluvial bedrock erosion are used to simulate feedbacks between mountain growth, lithospheric deformation, and global climate change (e.g., Willett, 1999); the structure of mountain belts (e.g., Howard, 1994); and the spacing of hills and valleys (e.g., Perron et al., 2008). Inversely, these models are used to reconstruct the tectonic and uplift history of continents (e.g., Whipple, 2004; Kirby and Whipple, 2012; Roberts et al., 2012; Croissant and Braun, 2014), decipher the imprint of glaciation and precipitation on topography (e.g., Brocklehurst and Whipple, 2007; Ferrier et al., 2013), and quantify the history of rainfall on Titan (Black et al., 2012) and on early Mars (e.g., Howard, 2007). The vast majority of these models drive landscape change through simple rules for river incision into bedrock by assuming that fluvial erosion rates (E) are a function of drainage area and local channel slope, often referred to as the stream-power erosion model (Howard and Kerby, 1983),

$$E = KA^m S^m \tag{1}$$

where A is the drainage area; S is the channel slope; and K, m, and n are empirical constants. Recent developments in exposure-age dating have revealed that catchment-averaged erosion rates (which typically average over 10^3 to 10^4 years) tend to follow Eq. (1) but that the coefficients in Eq. (1) vary widely in different landscapes (e.g., Ouimet et al., 2009; DiBiase et al., 2010), often attributed to differences in rock type and climate. These findings cast doubt on the predictive power of Eq. (1) outside of the landscapes and time scales for which the model has been calibrated.

To build more robust predictive models, the past 15 years have seen a surge in research focused on advancing new theory for the rate of bedrock river incision that attempts to incorporate the mechanics of specific erosion processes while remaining computationally tractable for landscape evolution simulations over geologic time. Much of the new insight to drive quantitative theory has come from simulating bedrock erosion in laboratory flume experiments, where bedrock erosion and channel evolution in the laboratory manifest over hours to weeks rather than the thousands of years that would be required to observe equivalent dynamics in nature. Outside of a few rare, extreme events (e.g., Lamb and Fonstad, 2010; Cook et al., 2013), annual-to-decadal observations of fluvial bedrock erosion in nature are limited to millimeters-to-centimeters of change (Fig. 1), resulting in negligible channel evolution and precluding direct observations of long-term feedbacks between water flow, sediment transport, bedrock erosion, and channel form. In contrast, flume experiments now allow direct measurements of these feedbacks through the development of erodible bedrock simulants and downscaling channel size that together speed the pace of bedrock erosion and channel evolution.

This paper is a synthesis of some of the key new developments in the mechanics of fluvial bedrock erosion from flume experiments, including new theories that have emerged as a result of experimentation. The paper is mostly a review of previous work; however, we do offer a few new ideas on bedrock erosion mechanics including bedrock-strength scaling, entrainment thresholds for plucking, and an assessment of bedrock analogs for experimentation. We focus solely on the mechanics of abrasion of rock by impacting fluvially transported particles and plucking of blocks of fractured rock. We focus on these two processes because they are arguably the most important erosion processes in bedrock rivers (e.g., Hancock et al., 1998; Whipple et al., 2000), they have received the most attention in recent experiments, and they have not been covered in detail in other review papers (Thompson and Wohl, 1998; Paola et al., 2009; Whipple et al., 2013). Consequently, a number of important processes are not within the scope of this paper. These processes include cavitation and groundwater sapping that have been suggested to play a role in bedrock-river erosion but to date lack conclusive field evidence (Whipple et al., 2000; Lamb et al., 2006). Entrainment of cohesive bed sediment from clear-water flows has been studied extensively experimentally (e.g., Dzulynski and Sanders, 1962; Shepherd and Schumm, 1974; Annandale, 1995; Brooks, 2001), but application of these results to bedrock rivers is unclear because rock erosion typically involves brittle fracturing (Engle, 1978). Corrosion, the collective weathering processes that weaken rock fabric and joints, is important in fluvial bedrock erosion, but to date has received little study experimentally (Hancock et al., 2011; Small et al., 2012; Whipple et al., 2013). Debris flows also erode bedrock channels, and there is growing work on debris-flow erosion mechanics from experiments (e.g., Hsu et al., 2008). Finally, a number of exciting experimental studies have been conducted to simulate the large-scale response of drainage basins or mountain ranges to climatic and tectonic forcing through use of sediment tables with tightly packed noncohesive sediment, rainfall misters, and base-level control (e.g., Hasbargen and Paola, 2000; Bonnet and Crave, 2003; Lague et al., 2003). These studies do not explicitly include the mechanics of abrasion and plucking, and we refer the reader to Paola et al. (2009) for a recent review.

With our focus set on the mechanics of abrasion and plucking from experiments and theory, we first discuss some of the issues in scaling laboratory experiments focusing on the relationship between rock strength and rock erodibility, which ultimately opens the door to quantitative-scaled experiments of bedrock erosion by abrasion. Second, we discuss how zero-dimensional bedrock abrasion experiments reveal a dominant and dual role of sediment supply in setting the rate of erosion, including the importance of bedload and of suspended sediment. Third, we review experiments that reveal strong feedbacks

Please cite this article as: Lamb, M.P., et al., New insights into the mechanics of fluvial bedrock erosion through flume experiments and theory, Geomorphology (2015), http://dx.doi.org/10.1016/j.geomorph.2015.03.003

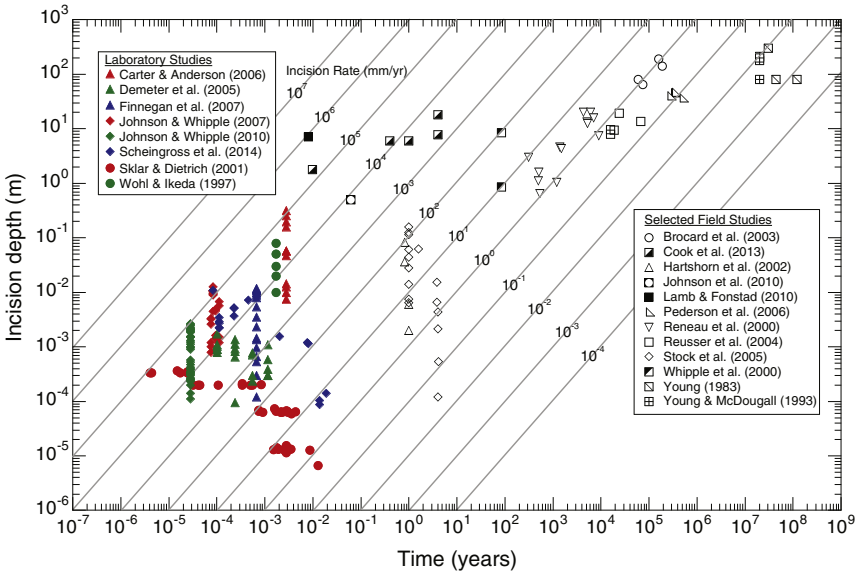

Fig. 1. Length and time scales for laboratory and field measurements of bedrock incision rates. Laboratory experiments reproduce a wide range of incision rates observed in the field but at vastly reduced length and time scales. Shorter measurement time intervals are due to lack of intermittency and use of weak bedrock analog materials; smaller incision depth measurements are possible because of controlled conditions and high-precision measurement techniques. Data sources include the following otherwise uncited works: Johnson et al. (2010); Pederson et al. (2006); Reneau (2000); Reusser et al. (2004); Stock et al. (2005) and Young (1983).

between channel form, bed roughness, sediment supply, and rock abrasion. Fourth, we derive new entrainment thresholds for block plucking by vertical entrainment, sliding, and toppling and compare these expectations to available experimental observations. Fifth, we discuss briefly the mechanics of abrasion and plucking at waterfalls. Finally, we identify a number of promising areas for future experimentation.

2. Scaling laboratory experiments for bedrock erosion

Laboratory experiments provide a means to test hypotheses that are difficult to test in natural rivers because in the lab specific mechanisms and functional relationships between variables can easily be isolated. However, experiments are inherently limited to the length scales that can be accommodated in a laboratory facility and to the time scales over which experiments can be completed. Applying knowledge gleaned from controlled experiments to field settings thus requires scaling relationships that apply across a wide range of length and time scales. As illustrated in Fig. 1, incision rates measured in the field vary over nine orders of magnitude, from the equivalent of 10^6 mm/y in a single dam release flood (Lamb and Fonstad, 2010), to 10^{-3} mm/y estimated over hundreds of million years of landscape evolution in Australia (Young and McDougall, 1993). Incision rates measured in the lab span nearly as wide a range; however, the length and time scales are much smaller.

Working at these smaller scales has advantages. Reduced size permits work at different dimensions, including fully three-dimensional channels (Wohl and Ikeda, 1997; Carter and Anderson, 2006; Finnegan et al., 2007), two-dimensional wide fixed-wall (Johnson and Whipple, 2007, 2010), one-dimensional narrow fixed-wall (Taki and Parker, 2005), and essentially zero-dimensional abrasion mills (Sklar and Dietrich, 2001; Scheingross et al., 2014). Measurements of erosion depths can be more precise under laboratory conditions, for example by using laser scanning or mass differencing of samples small enough for precision balances. The trade off, however, is that the magnitude of erosive forces is much less.

Big differences between experiments and natural rivers arise when comparing the time scale of erosion. For example, Sklar and Dietrich (2001) and Brocard et al. (2003) measured incision rates of ~1 mm/yr (Fig. 1), but the time scale between lab and field measurements differed by seven orders of magnitude. Equivalent rates in the lab, despite smaller scales, are caused by two effects: the lack of intermittency and use of weak materials that erode more rapidly for a given intensity of erosive attack. Lab experiments in effect simulate flood conditions when incision and other morphologic changes occur. In the field, these flows could happen <1% of the time (Sklar and Dietrich, 2006) or much less frequently (e.g., Baker and Pickup, 1987). Moreover, field incision rates over long time spans may include periods of aggradation when even large floods cause no incision (Finnegan et al., 2014). Time intervals with no vertical incision may still be important to morphologic evolution of bedrock channels because of channel-wall erosion and reduction of rock strength by weathering; however, the latter is difficult to capture experimentally.

The shorter time scales and length scales of most laboratory experiments as compared to natural bedrock rivers pose a number of challenges and considerations for scaling. Experiments aimed at understanding the basic mechanics of transport processes typically follow classic dynamic scaling where key dimensionless variables, like the Reynolds number (Re) are either matched between experiment and nature or are designed to be within the same regime where dynamics are similar. Strategies for dynamic scaling of hydraulic and sediment transport experiments have been discussed at length previously (e.g., Yalin, 1977; Peakall et al., 1996), and we review some of the key concepts in Section 2.1. Bedrock erosion experiments pose an additional challenge in that bedrock material properties and erodibility also must be considered in scaling, and workers in the last 15 years have made progress identifying and testing dimensionless variables for bedrock erosion (discussed in Sections 2.2 and 2.3). In Section 2.4 we introduce scaling concepts for bedrock erosion by plucking, and in Section 2.5 we briefly discuss the importance of channel-scale dimensionless variables in designing experiments aimed at morphodynamic interactions.

2.1. Scaling hydraulics and sediment transport

Like laboratory alluvial channels, quantitative scaling of experimental bedrock channels requires relationships for characterizing flow conditions and interactions between water and sediment. These are well developed from the long history of experimental work on hydraulic modeling and sediment transport (Yalin, 1977; Peakall et al., 1996). Two fundamental nondimensional numbers are used to compare hydraulic conditions between laboratory models and field prototype channels. The Reynolds number quantifies the ratio of turbulent to

Please cite this article as: Lamb, M.P., et al., New insights into the mechanics of fluvial bedrock erosion through flume experiments and theory, Geomorphology (2015), http://dx.doi.org/10.1016/j.geomorph.2015.03.003

viscous forces in the flow:

$$\mathrm{Re} = \frac{\rho_w U h}{\mu} \tag{2}$$

in which ρ_w is the density of water, U is the depth-averaged mean flow velocity, h is mean flow depth, and μ is the dynamic fluid viscosity. The Froude number (Fr) quantifies the ratio of inertial to gravitational forces

$$\mathrm{Fr} = \frac{U}{\sqrt{gh}} \tag{3}$$

where g denotes the acceleration of gravity. Eq. (3) also represents the ratio of the flow velocity to the speed of a surface wave in shallow flow.

In scaling down from nature to lab, matching both Re and Fr generally is not feasible. Fortunately, Re does not need to match for dynamic similarity; researchers have shown that for fully turbulent flow ($\mathrm{Re} > \sim 10^3$), the vertical structure of steady and uniform unidirectional flow is self-similar and follows

$$\frac{u(z)}{u_*} = \frac{1}{\kappa} \ln \frac{z}{z_0} \tag{4}$$

where u is the time-averaged flow velocity, $u_* = \sqrt{\tau_b/\rho_w}$ is the bed shear velocity, τ_b is the bed shear stress, $\kappa = 0.41$ is von Karman's constant, z is the height above the bed, and z_0 is an empirical constant that depends on whether the bed is hydraulically rough or smooth (e.g., Schlichting, 1979). For the case of a hydraulically rough bed, which is likely the case in most natural rivers with gravel or larger bed roughness (e.g., Parker, 1991; Parker et al., 2007), $z_0 = k_s/30$ and k_s is the bed roughness length scale. Thus, for fully turbulent and hydraulically rough flows, flow velocity is independent of the Reynolds number and fluid viscosity. This makes laboratory experiments using water flows also applicable to different gravities and rivers of more exotic fluids, such as brines on Mars (Lamb et al., 2012; Grotzinger et al., 2013) or methane rivers on Titan (Perron et al., 2006; Burr et al., 2013), as long as they are also Reynolds-number independent. Most bedrock erosion experiments to date have been conducted in the turbulent regime (Fig. 2), except for those aimed at landscape-scale dynamics that did not explicitly investigate abrasion or plucking (e.g., Hasbargen and Paola, 2000; Bonnet and Crave, 2003; Lague et al., 2003).

The threshold value of $\mathrm{Fr} = 1.0$ separates supercritical flow ($\mathrm{Fr} > 1$) from subcritical flow ($\mathrm{Fr} < 1$). In engineering scale models of particular flow configurations, Fr should match for dynamic similitude. Most bedrock erosion experiments to date have been in the supercritical regime (Fig. 2). In the field, Fr during active bed erosion is not well known, in part because the discharge at which most incision occurs depends on many factors, including sediment supply and grain size (Sklar and Dietrich, 2006). Surface waves and other indicators of supercritical flow are often observed in bedrock channels (e.g., Richardson and Carling, 2006), leading to the common assumption that supercritical flow is characteristic of incising bedrock channels (Tinkler and Wohl, 1998).

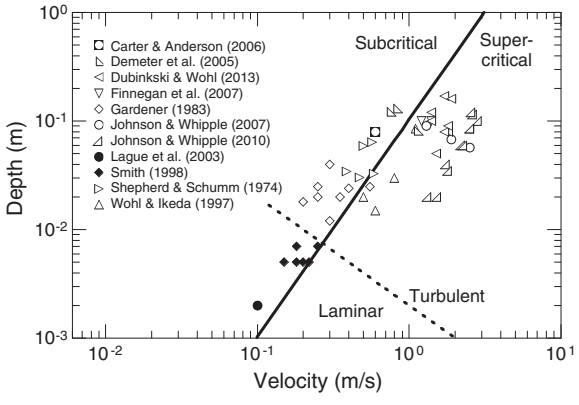

Fig. 2. Hydraulic regimes of laboratory bedrock channel experiments. Solid line represents the threshold between subcritical and supercritical flow ($\mathrm{Fr} = 1$); dashed line represents the threshold between laminar and turbulent flow ($\mathrm{Re} = 2000$). Data sources include the following otherwise uncited works: Smith (1998).

Several nondimensional numbers are used for scaling interactions between water and sediment. The Shields number quantifies the ratio of bed stress caused by fluid drag on a particle to the submerged particle weight per unit area,

$$\tau^* = \frac{\tau_b}{(\rho_s - \rho_w) g D} \tag{5}$$

in which ρ_s is the sediment density, and D is the particle diameter. The threshold of sediment motion is expressed as a critical value, τ_c^*, which for the median grain size varies primarily as a function of particle size (through the particle Reynolds number, Re_p) and channel slope (or equivalently flow depth relative to sediment size) (e.g., Buffington and Montgomery, 1999; Lamb et al., 2008c). The particle Reynolds number describes the balance between viscous and turbulent effects in the boundary layer around the particle,

$$\mathrm{Re}_p = \frac{\rho_w u_* D}{\mu}. \tag{6}$$

For example, particle drag coefficients (C_D) and the critical Shields number (τ_c^*) have been found to be independent of Re_p and sediment size for $\mathrm{Re}_p > \sim 10^2$ (equivalent to gravel or coarser sediment) in a manner similar to Reynolds-number independence for velocity in fully turbulent flows. This makes gravel, for example, a good scale analog for boulders in natural rivers. For gravel-bedded and low gradient ($S < 1\%$) rivers, τ_c^* is about 0.045 (Shields, 1936; Brownlie, 1983; Wilcock, 1993). The critical Shields stress can range up to $\tau_c^* = 0.2$ for very steep channels (Lamb et al., 2008c; Scheingross et al., 2013; Prancevic et al., 2014) and can be $\ll 0.01$ for isolated grains on smooth bedrock beds (Hodge et al., 2011; Chatanantavet et al., 2013).

At high transport stages (i.e., τ^*/τ_c^*), the Rouse number (Z) becomes important,

$$Z = \frac{w_s}{\kappa u_*} \tag{7}$$

in which w_s is the particle fall velocity. Generally particles transition from the bedload-transport regime to the suspension regime when the ratio u_*/w_s exceeds unity ($Z < 2.5$) (Bagnold, 1966). These two regimes result in different particle trajectories (Fig. 3), different particle–bedrock interactions, and consequently different bedrock erosion rates (explored in Section 3.2).

In sediment transport experiments, achieving dynamic similarity for hydraulics and for sediment transport is often difficult. For example, experiments can produce fully turbulent open-channel flows with flow depths scaled down by orders of magnitude from natural rivers (Fig. 2). Sediment size, however, cannot be scaled down by a commensurate amount because small sediment sizes may produce particle Reynolds numbers that fall below $\mathrm{Re}_p \sim 10^2$; and even more important, other processes such as cohesion become important for mud. Consequently, alluvial bed slopes tend to be steep in experiments in order to achieve sediment transport despite relatively coarse sediment and shallow flows. Steeper slopes, in turn, often cause Fr to be larger than in natural rivers. One solution to these issues has been to use low density sediment, such as walnut shells or plastic beads, in laboratory experiments to produce transport on lower bed slopes (e.g., Chatanantavet and Lamb, 2014). This is an effective strategy for alluvial river experiments, but low-density sediment and sub-sand-sized particles pose an issue for bedrock-erosion experiments because particle-bed impacts must have sufficient kinetic energy to produce measurable erosion

Please cite this article as: Lamb, M.P., et al., New insights into the mechanics of fluvial bedrock erosion through flume experiments and theory, Geomorphology (2015), http://dx.doi.org/10.1016/j.geomorph.2015.03.003

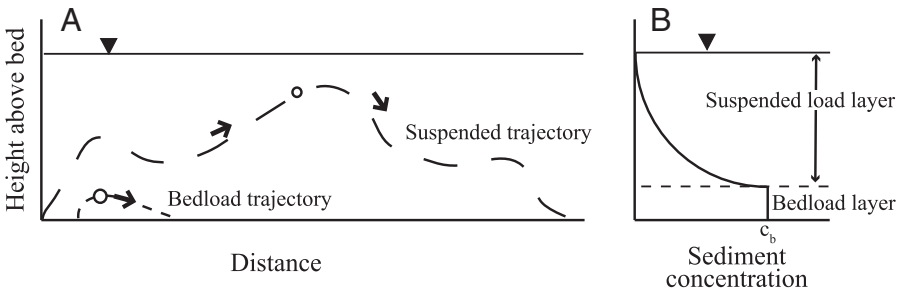

Fig. 3. (A) Schematic cartoon of individual particle trajectories for sediment in the bedload regime where particles follow ballistic trajectories and for sediment in the suspension regime where trajectories are controlled by fluid turbulence. (B) Schematic plot of sediment concentration versus height within the suspension-regime. Sediment concentration increases toward the bed (Rouse, 1937); and the near-bed sediment concentration, c_b, is assumed constant throughout the entire bedload layer.
(A) Modified from Francis (1973).

rates. Experiments indicate that particles also must have sufficiently large particle Stokes numbers (St),

$$\mathrm{St} = \frac{\rho_s w_i D}{9\mu} \tag{8}$$

for bedrock erosion to occur (Scheingross et al., 2014), where w_i is the particle impact velocity. Experiments measuring the rebound of spherical and natural particles against planar beds suggest that particle impacts are viscously damped when collisions fall below particle Stokes numbers of ~10^1–10^2 (e.g., Joseph et al., 2001; Schmeeckle et al., 2001; Joseph and Hunt, 2004; Li et al., 2012).

2.2. Bedrock simulants in abrasion experiments

Only a few laboratory experiments have eroded natural rock (Sklar and Dietrich, 2001; Small et al., 2012; Wilson and Lavé, 2014). Instead, the majority of experimentalists choose to use bedrock analogs in place of natural rock in erosional experiments. Bedrock analogs can offer advantages over natural rock including faster rates of erosion, ease of shaping or molding the bed into a desired configuration, and the ability to be made in the laboratory or supplied commercially. Several analog materials have been used, including cohesive sediments, concrete, and polyurethane foam. The most suitable material analogs are those that replicate the deformation and wear behavior of natural rock as close as possible, allow for erosion rates sufficiently fast to be observable over experimental time scales, and follow scaling laws that can be used to relate laboratory erosion rates to field time scales.

Beginning with the pioneering experiments of Schumm et al. (1987), many laboratory investigations have used clay-based bedrock analog materials to accelerate incision and morphologic evolution. Clay added to mixtures of silt and fine sand provides cohesion sufficient to form vertical walls (Shepherd and Schumm, 1974; Gardner, 1983; Wohl and Ikeda, 1997) and, when subject to flowing water and sediment, produces sculpted bedforms such as flutes and potholes (Dzulynski and Sanders, 1962). Although the morphologies formed in clay-silt cohesive materials may be similar to features found in hard crystalline rock (e.g., Wohl and Ikeda, 1997), quantitatively scaling the erosion rates and flow conditions to the field is challenging because the material deforms plastically and fails to reproduce the brittle behavior of natural rock. These two limitations make it difficult to test bedrock incision theories (e.g., Sklar and Dietrich, 2004); however, cohesive sediment mixtures are likely excellent analogs for lowland rivers that have recently been shown to incise into consolidated mud (e.g., Nittrouer et al., 2011; Shaw et al., 2013).

The past ~15 years have seen a shift toward the use of weak concrete as a bedrock analog instead of cohesive sediments (e.g., Sklar and Dietrich, 2001; Demeter et al., 2005; Carter and Anderson, 2006; Finnegan et al., 2007; Johnson and Whipple, 2007, 2010). Unlike cohesive sediments, concrete is brittle and has been shown to erode following the same tensile-strength scaling as observed in natural rock (Sklar and Dietrich, 2001). Concrete is similar in many respects to clastic sedimentary rocks, and by varying particle sizes in concrete mixtures experimenters can approximate natural rocks ranging from siltstones to conglomerates. The tensile strength of concrete can be easily controlled by changing the ratio of sand to cement in the mixture, allowing workers to adjust erosion resistance. As with cohesive sediment mixtures, concrete produces erosional morphologies that are similar to erosional rock bedforms in natural channels (e.g., Finnegan et al., 2007; Johnson and Whipple, 2007). Because concrete is initially in a fluid state, it can be set in molds to produce desired morphologies, such as regular roughness patterns (Davis, 2013). The main limitation of concrete is that it requires long curing times. Concrete cures following a logarithmic time scale, typically taking more than 1 month to reach its final tensile strength (Nelson, 2003), although this time can be reduced by additives that accelerate curing. For example, Type III Portland cement reaches 70% of its ultimate strength in 3 days (Kosmatka et al., 2002); rapid curing cements were used in making analog bedrock by Hsu et al. (2008) and Fuller (2014). Because the change in tensile strength is initially rapid, achieving a constant tensile strength over the length of laboratory experiments (which may take multiple days or weeks to run), requires pouring concrete days to weeks in advance of starting experiments.

Recently, closed-cell polyurethane foam has been explored as an alternative bedrock analog for abrasion (Scheingross et al., 2014). Foam has been successfully used as a bedrock analog in studies examining abrasion by wind-transported sediment, with results showing similar morphologic patterns of erosion between foam and rock (Bridges et al., 2004; Laity and Bridges, 2009). In fluvial abrasion experiments, foam has been shown to follow the same tensile-strength scaling as rock and concrete (Scheingross et al., 2014) and produces erosional morphologies consistent with those observed in nature. Foam can be easier to work with than concrete or cohesive sediment mixtures as it requires no curing time, can be purchased commercially in a variety of tensile strengths, and its low density makes it easy to transport. However, foam also has disadvantages compared to concrete. Foam is 20–40 times more costly per unit volume and is supplied by the manufacturer in rectangular blocks and must be user-shaped. In addition, while foam breaks in a brittle manner, it can also deform plastically under high energy sediment impacts, although in most experiments impact energy will be below the threshold of plastic deformation. For example, we found that when dropping particles from rest through 6 cm of water, particles $D > 2.5$ cm were needed to produce plastic deformation in 0.32 MPa tensile strength foam; this coarse gravel is larger than the grain sizes typically used in most bedrock abrasion experiments.

A final consideration in the choice of bedrock material analog is the role of eroded material. Foam is low-density and erodes in submillimeter pieces such that eroded foam is transported away in washload and does not produce further erosion. This is unlike concrete or cohesive sediment mixtures where the sand liberated in erosion can produce further

Please cite this article as: Lamb, M.P., et al., New insights into the mechanics of fluvial bedrock erosion through flume experiments and theory, Geomorphology (2015), http://dx.doi.org/10.1016/j.geomorph.2015.03.003

erosion depending on the size of sand used and the hydraulics of the particular experiment.

2.3. Scaling rock resistance to abrasion

In the stream power model (Eq. (1)), the *erodibility* or *erosivity* coefficient K is assumed to capture rock susceptibility to erosion. However, in practice, K is a lumped parameter that also subsumes many other factors, including channel geometry, hydraulic roughness, sediment flux and grain size, magnitude-frequency tradeoffs, and the efficiency of multiple potential detachment mechanisms (Sklar and Dietrich, 1998; Whipple, 2004). As a result, K cannot be readily scaled between laboratory and field channels and has ambiguous physical meaning even when comparing field sites at similar scales (Stock and Montgomery, 1999; Kirby and Whipple, 2001).

Physically explicit measures of rock resistance to erosion should differ depending on the dominant mechanism for rock detachment. For rock wear by sediment impacts, arguably a ubiquitous and frequently dominant mechanism, Sklar and Dietrich (2001) demonstrated experimentally that mass erosion rate (E_m) scales with the inverse square of rock tensile strength (σ_T):

$$E_m = E_o\left(\frac{\sigma_T}{\sigma_0}\right)^{-2} \tag{9}$$

in which E_o is the expected erosion rate at a reference tensile strength σ_0(Fig. 4A). In these experiments, 20-cm-diameter rock disks were eroded by sediment impacts at the base of vertically oriented cylinders, or abrasion mills, that contained water and sediment circulated by motor-driven propellers (Fig. 4D). Tensile strength was measured with the Brazilian splitting tensile strength test (ISRM, 1978). Rock types tested spanned the range of strengths of rocks found in the field, from very strong andesite and quartzite ($\sigma_T > 20$ MPa) to weak mudstones and weathered sandstones ($\sigma_T < 0.1$ MPa). Sklar and Dietrich (2001) also found that disks of weak concrete, made from Portland cement and fine sand in various ratios, followed the same inverse square scaling relation between erosion rate and tensile strength.

Although the scaling of erosion rate with the inverse square of tensile strength has now been confirmed by several experiments (Sklar and Dietrich, 2001; Hsu et al., 2008; Scheingross et al., 2014), a satisfactory theoretical explanation remains the subject of ongoing work. Resistance to impact wear in brittle materials can be related to toughness, the capacity to store energy through elastic strain (Engle, 1978). At the limit of brittle failure, the strain energy per unit volume (β) scales with σ_T^2 divided by Young's modulus of elasticity (Y). On this basis, Sklar and Dietrich (2004) proposed that rock resistance to wear by sediment impacts could be quantified as the impact energy required to detach a unit volume (ε_v),

$$\varepsilon_v = k_v\beta = k_v\frac{\sigma_T^2}{Y} \tag{10}$$

where k_v is a dimensionless coefficient that depends in part on the efficiency of energy transfer. Sklar and Dietrich (2004) determined k_v to be ~10^6 by dropping gravel clasts from known heights and measuring the resulting volumetric wear of rock disks of various strengths (Sklar and Dietrich, 2004, 2012). However, they assumed a constant value for $Y = 5 \times 10^5$ MPa, hence the empirical calibration of Eq. (10) can be written as

$$\varepsilon_v = \frac{\sigma_T^2}{k_Y} \tag{11}$$

where the dimensional coefficient k_Y ~ 2 MPa and includes the effects of elasticity. To explore the influence of elasticity on rock resistance to abrasion, Beyeler and Sklar (2010) measured Young's modulus and several other rock properties for a large subset of the rock disks eroded by Sklar and Dietrich (2001) and found that erosion rates scale with $\beta^{-1.5}$. However, compared to tensile strength alone, including Y in the regression substantially increased the scatter and reduced the predictive power of the relationship.

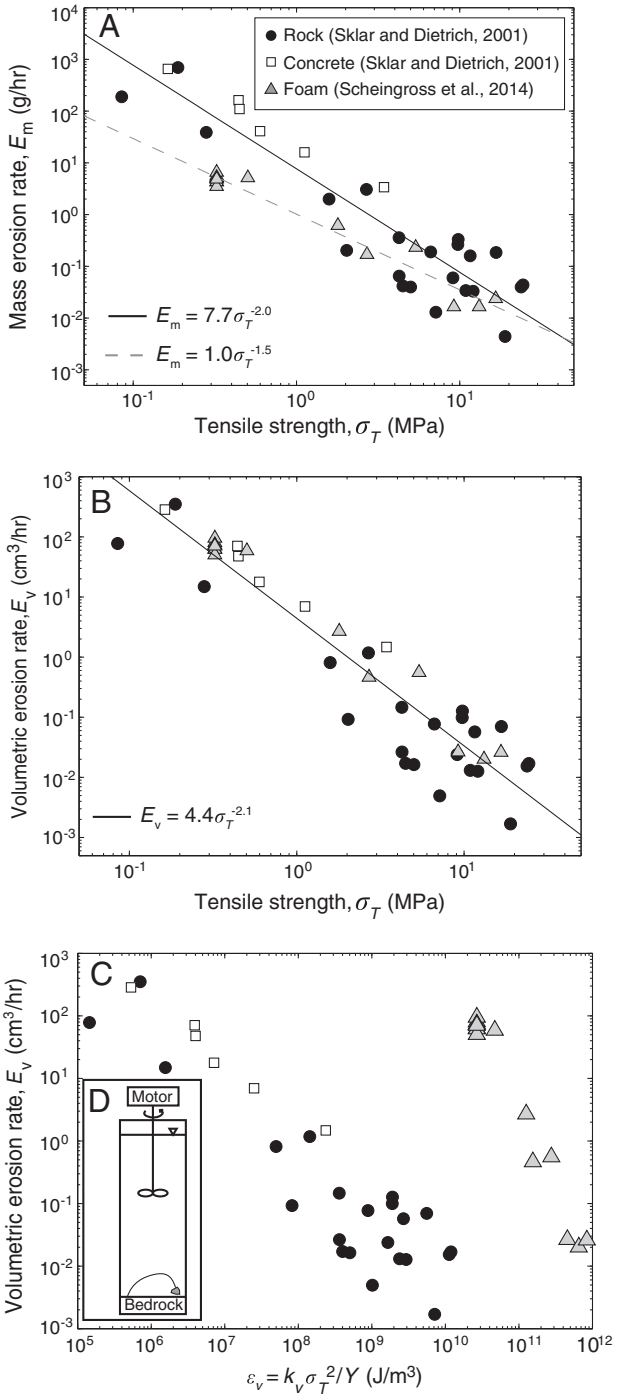

Fig. 4. Compilation of abrasion mill erosion rates for natural rock, concrete, and foam. (A) Mass erosion rate versus tensile strength with lines showing fits to rock and concrete data (solid line) and foam data (dashed line). (B) Volumetric erosion rate versus tensile strength with solid line showing best fit to rock, concrete, and foam data. (C) Volumetric erosion rate versus ε_v (Eq. (10)) with $k_v = 10^6$. (D) Schematic of the abrasion mills used in Sklar and Dietrich (2001) and Scheingross et al. (2014).

Scheingross et al. (2014) replicated the experimental set up of Sklar and Dietrich (2001) using a rigid, polyurethane foam substrate in place of rock or concrete. The polyurethane foam spans the same range of

Please cite this article as: Lamb, M.P., et al., New insights into the mechanics of fluvial bedrock erosion through flume experiments and theory, Geomorphology (2015), http://dx.doi.org/10.1016/j.geomorph.2015.03.003

tensile strengths (~10^{-1} to 10^{1} MPa) as natural rock, but varies approximately an order of magnitude in bulk material density (ρ_r) and two orders of magnitude in Young's modulus. To the extent that polymer-based foam obeys the same fracture mechanics as crystalline rock, the Scheingross et al. (2014) experiments can be used to test aspects of the erosion theory (i.e., Eq. (10)) in ways that cannot be done with natural rock or concrete that have little variation in ρ_r and Y.

Foam mass erosion rates have a slightly different power-law scaling with tensile strength than observed in rock or concrete (Fig. 4A); however, volumetric erosion rate (E_v) for all three materials follow identical scaling with $E_v = E_m/\rho_r$ proportional to ${\sigma_T}^{-2}$ (Fig. 4B). This is in agreement with the formulations of Bitter (1963) and Sklar and Dietrich (2004) that are based on a finite volume of erosion for a given impact energy. A volumetric, rather than mass-based, erosion law may be more appropriate for brittle material such as rock, where erosion occurs by the formation and coalescing of cracks (Engle, 1978). When plotted against strain energy, foam volumetric erosion rates differ greatly from rock and concrete because the Young's modulus of foam is orders of magnitude lower than rock for a given tensile strength (Fig. 4C). This result implies that for Eq. (10) to apply to both rock and foam, k_v must vary proportionally with Y, which is contrary to the theoretical expectation of constant k_v (Engle, 1978). Together with the results of Beyeler and Sklar (2010), the foam results suggest that the relationship between erosion rate and tensile strength is not improved by including Young's modulus as an independent factor. This may reflect the fact that strength and elasticity are strongly correlated, as are most other rock material properties, including bulk density and compressive strength. As a result, erosion resistance could be indexed by measurements of other rock properties besides tensile strength, including elasticity, which underlies the common use of the Schmidt hammer to characterize relative rock resistance in the field (Goudie, 2006).

A better theoretical foundation for scaling rock resistance to erosion by particle impacts may be provided by fracture toughness (K_{IC}), which quantifies the material resistance to propagation of fractures that originate from preexisting flaws (or 'cracks') of length c,

$$K_{IC} = (\pi c)^{0.5}\sigma_T \tag{12}$$

in which the subscript IC denotes open mode tensile loading at the crack tip (Lawn, 1993). Preexisting flaws in rock are provided by boundaries between mineral grains in crystalline rock, between clasts and cement in clastic sedimentary rocks (e.g., Hatzor and Palchik, 1997), as well as between micropores and other discontinuities in rock fabric. To investigate the role of flaw size, Beyeler and Sklar (2010) measured crystal and clast size (D_c) in thin sections of disks eroded by Sklar and Dietrich (2001) and found that grain size, together with porosity (p), explained a large fraction of the scatter in the fit between erosion rate and tensile strength present in Fig. 4B.

Improved understanding of the scaling between rock material properties and resistance to erosion by low velocity sediment impacts would also help inform studies of incision into surfaces of other planetary bodies, particularly outer solar system icy satellites such as Titan. There, where surface temperature is ~90 K, channels may be actively incising into Titan's water–ice bedrock by flows of liquid methane carrying water–ice clasts as bedload (Collins, 2005; Perron et al., 2006; Burr et al., 2013). To extend rock erosion resistance scaling to ultracold ice, Litwin et al. (2012) measured the tensile strength and fracture toughness of polycrystalline ice across a temperature range spanning −10 °C to −150 °C and found ice tensile strength scales linearly with temperature, with the strength of ice at Titan temperatures roughly double that of terrestrial conditions. In a complementary laboratory study, Sklar et al. (2012) measured volumetric erosion rates of ultracold ice subjected to particle impacts and found that the impact energy required to erode a unit volume of ice was roughly equal to that measured by Sklar and Dietrich (2004) for natural rock of similar tensile strength.

In summary, experiments suggest that rates of bedrock incision by particle impacts can be scaled across a range of rock types and strengths, including analog bedrock materials and ultracold ice, using

$$E = \frac{q_e}{\varepsilon_v} = \frac{q_e k_R}{\sigma_T^2} \tag{13}$$

in which q_e is the flux of impact kinetic energy per unit bed area, and the dimensional coefficient k_R is a function of other rock properties, i.e., $k_R = f(D_c, p, \rho_r, Y)$. Eq. (13) shows how incision rates can be accelerated in the lab relative to the field by a factor of 10^6 or more (Fig. 1), i.e., where laboratory bedrock tensile strength is weaker by a factor of 10^3 or more (Fig. 4). Moreover, with Eq. (13) it is possible to distinguish the effects of rock resistance to erosion from intermittency in temporal scaling between lab and field and to isolate erosion resistance from the effects of differing erosional intensity, as represented by q_e.

2.4. Scaling bedrock incision by plucking

In comparison to abrasion, much less work has been done on fluvial bedrock erosion by plucking, including how to properly scale such experiments. Plucking involves the removal of large chunks of rock along intersection joint planes, and it may dominate erosion rates in well-jointed rock types (e.g., columnar basalt) and during large floods that are capable of entraining and transporting large blocks (e.g., Malde, 1968; Baker, 1973; Lamb and Fonstad, 2010; Lang et al., 2013; Lamb et al., 2014). Bedrock joints can be primary (e.g., cooling joints in basalt) or secondary (e.g., tectonic- and topographic-induced fractures; Miller and Dunne, 1996; Martel, 2006; Clarke and Burbank, 2010). Fluid flow and sediment-transport processes can also contribute to fracturing rock or loosening of preexisting joints through chemical and physical weathering, hydraulic wedging of sediment into crack openings (Hancock et al., 1998), crack development from saltating clasts, and hydraulic pressure fluctuations (Hancock et al., 1998; Whipple et al., 2000).

The physics of how rock came to be fractured at Earth's surface are not well understood, and the few plucking experiments that have been conducted have focused instead on the hydraulic removal of already-fractured rock (e.g., Coleman et al., 2003; Dubinski and Wohl, 2013). Under the special case of little to no interlocking or friction between blocks of rock, plucking is seemingly analogous to bedload transport of noncohesive sediment (e.g., Chatanantavet and Parker, 2009; Lamb and Fonstad, 2010). If this is the case, then successful scaling relationships for plucking are likely to be similar to those for sediment transport, including a critical Shields number of block entrainment and a block-Reynolds number (cf. Eqs. (5) and (6)). However, for the case of plucking, the characteristic length scales in the dimensionless numbers may vary depending on block aspect ratios and whether the dominant process is vertical entrainment, sliding, or toppling (e.g., Hancock et al., 1998; Whipple et al., 2000). In Section 5 we formalize some of these ideas, propose dimensionless numbers for plucking thresholds, and compare results to existing experimental data.

2.5. Scaling morphodynamics

In experiments investigating morphodynamic interactions — in which evolving bed topography significantly influences the rates of water flow, sediment transport, and bedrock erosion — additional dimensionless numbers can be identified and used for scaling of system-scale dynamics (Paola et al., 2009; Ganti et al., 2014). For example, some bedrock rivers meander and experience loop cutoff, and these dynamics likely manifest over lengths that scale with the channel width and over times that scale with the time to erode laterally a channel width (e.g., Limaye and Lamb, 2014). Similarly, bedrock river channels may adjust their width in response to changes in sediment supply, and the rate of these changes may scale with the time for a river to incise

Please cite this article as: Lamb, M.P., et al., New insights into the mechanics of fluvial bedrock erosion through flume experiments and theory, Geomorphology (2015), http://dx.doi.org/10.1016/j.geomorph.2015.03.003

a characteristic channel depth (e.g., Finnegan et al., 2007). Thus, the faster erosion rates and smaller length scales in laboratory experiments (Fig. 1), as compared to natural rivers, allow experiments to be particularly effective in exploring morphodynamic interactions and channel-scale dynamics over tractable study times, dynamics in nature that are typically impossible to observe directly. Paola et al. (2009) addressed system-scale dimensionless variables for much larger erosional and depositional systems, where dimensionless numbers related to tectonics and climate are also important.

3. The role of sediment transport in bedrock abrasion in zero-dimensional experiments

In 1877, G.K. Gilbert articulated the fundamental but opposing influences that coarse sediment exerts on the process of river incision into bedrock (Gilbert, 1877). On the one hand coarse sediment supplies the abrasive tools that are required to sustain erosion (the *tools* effect). On the other hand, when deposited, coarse sediment protects the bed from abrasion (the *cover* effect). This realization frames Gilbert's hypothesis that intermediate sediment supplies, which optimize the tools and cover effects, result in the highest abrasion rates. Importantly, Gilbert's hypothesis also suggests that stream power-based approaches to modeling bedrock river incision are limited by the fact that they do not account for sediment supply directly. In other words, the dependence of river incision rate on sediment supply results in a nonunique relationship between river incision rate, channel slope, and drainage area (e.g., Sklar and Dietrich, 2004; Gasparini and Brandon, 2011).

3.1. Effect of sediment cover

The first test of Gilbert's hypothesis was accomplished experimentally by Sklar and Dietrich (2001). This study used experimental abrasion mills to simulate the wear of a planar bedrock river bed caused by bedload impacts (Fig. 4D). Sediment of various amounts and sizes was introduced into the mills. The shear stress of the circulating water acting on the coarse sediment led to the saltation of bedload across the surface of the bedrock disks. The results of these experiments demonstrate that peak bedrock erosion rates occur at an intermediate amount of coarse-grained sediment supply where the bedrock is only partially exposed on the bed (Fig. 5). The experiments thus provide direct support for Gilbert's hypothesis and, hence, for the limitations of using topographic data alone (e.g., Eq. (1)) to estimate incision rates and patterns. In addition to sediment supply, experiments have also revealed that erosion rates are highly sensitive to sediment size and transport mode.

3.2. Influence of particle size and trajectory

Particle size and transport trajectory bear a strong influence on fluvial bedrock abrasion rates by influencing the rate and kinetic energy of sediment impacts. The abrasion mill experiments of Sklar and Dietrich (2001) showed that, with all other variables held constant, erosion rates increased with increasing grain size caused by higher kinetic energy of impacts (Fig. 6). For very large particles, however, erosion rates dropped to zero because no particles were moving, and for small particles transported primarily in suspension erosion rates were relatively small (Fig. 6). Thus, in addition to the effects of *tools* and *cover*, bedrock abrasion can be separated into three regimes based on transport mode: bedload, suspension, and no motion.

The controls on particle motion have been the subject of laboratory experiments for over a century. Gilbert (1914) made detailed observation of the motion of particles in a 10-m-long flume, noting that particles near the bed move predominately by saltation (Fig. 3). Subsequent studies (e.g., Einstein, 1950; Francis, 1973; Abbott and Francis, 1977; Nino et al., 1994) made use of high-speed photography to analyze particle trajectories under variable shear stress and for sediment of different grain sizes, densities, and angularities. Using experimental data, Sklar and Dietrich (2004) showed that saltation hop length, height, and velocity follow a power-law scaling relationship with fluvial transport stage, τ^*/τ_c^*, suggesting that particle trajectory is controlled predominately by grain size, density, and fluid stress (Fig. 7). Chatanantavet et al. (2013) performed experiments analyzing grain motion over a smooth, Plexiglas bed and showed good agreement with the transport-stage power law scaling of Sklar and Dietrich (2004) — but only after adjusting the critical Shields stress value to account for a sediment-free bed (Fig. 7). Lower τ_c^* on smooth beds results

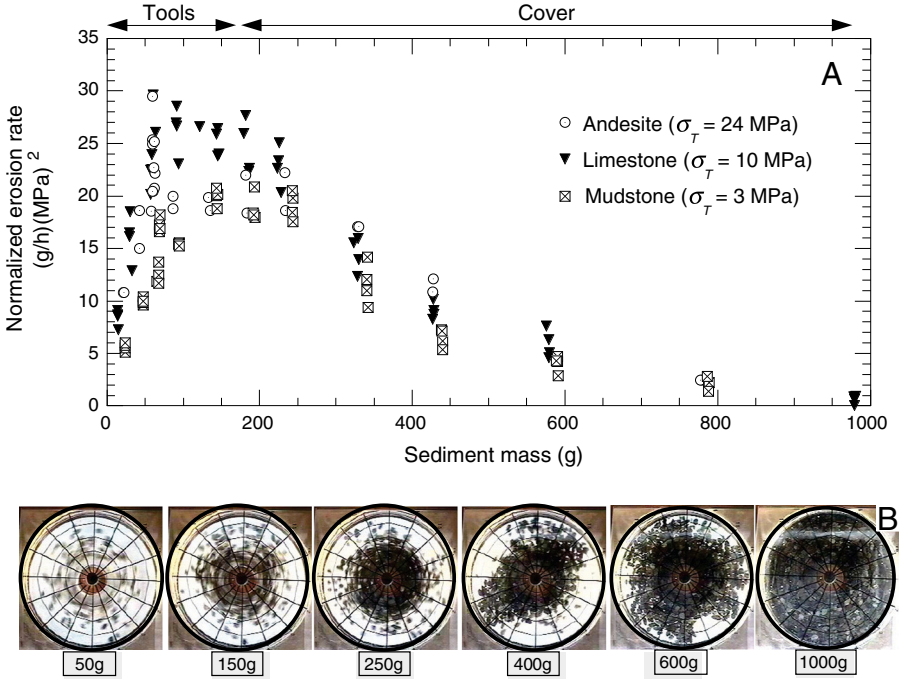

Fig. 5. (A) Variation in erosion rate with sediment loading (Sklar and Dietrich, 2001). Data for three rock types are collapsed by multiplying the erosion rate (g/h) by the square of rock tensile strength (MPa). (B) Variation in bed cover with increasing load imaged through the transparent floor of an abrasion mill.

Please cite this article as: Lamb, M.P., et al., New insights into the mechanics of fluvial bedrock erosion through flume experiments and theory, Geomorphology (2015), http://dx.doi.org/10.1016/j.geomorph.2015.03.003

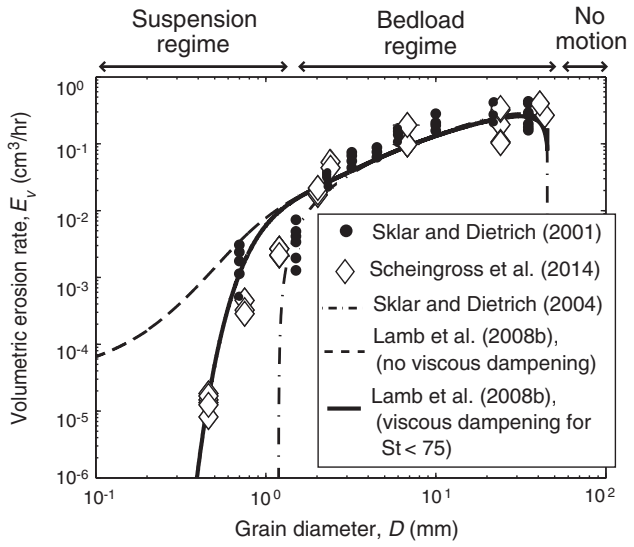

Fig. 6. Volumetric erosion rate, E_v, versus grain diameter, D, for abrasion mill experiments by Sklar and Dietrich (2001) and Scheingross et al. (2014). Lines show the theoretical predictions for the saltation–abrasion model and the total load model with and without viscous dampening.
Figure modified from Scheingross et al. (2014).

from the reduction in particle friction angle (e.g., Wiberg and Smith, 1987; Kirchner et al., 1990), and Chatanantavet et al. (2013) calculated τ_c^* as low as 0.007 for their experiments (compared to τ_c^* ~ 0.045 for rough beds). Chatanantavet et al. (2013) additionally showed that saltation hop height, length, and velocity could be well predicted by Fr-based scaling that is independent of transport stage for both smooth and rough beds, and this may provide an easier method to predict grain trajectories in bedrock streams where τ_c^* can be difficult to estimate. These ideas were formalized in a mechanistic model (Sklar and Dietrich, 2004; commonly referred to as the saltation–abrasion model), which expands on the form of Eq. (13) by parameterizing q_e for impacts by saltating bedload (Fig. 6). The good comparison between experiments and theory (Fig. 6) suggests that the observed decrease in erosion rates with smaller particle sizes in the abrasion mill experiments (with flow velocity and

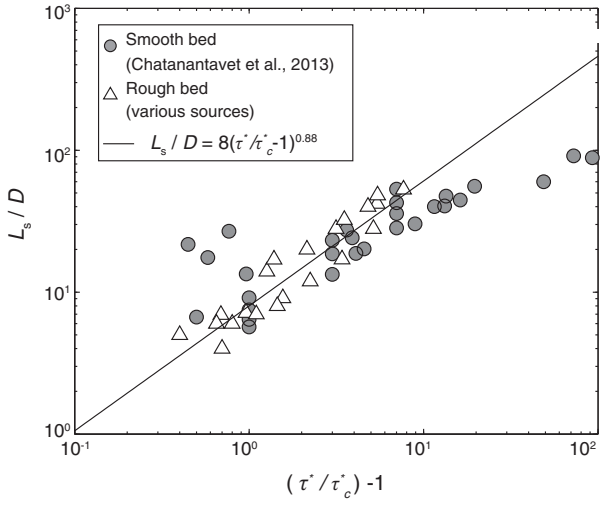

Fig. 7. Compilation of saltation hop length (L_s) normalized by grain diameter (D) versus excess shear stress. Line shows the empirical fit by Sklar and Dietrich (2004) that matches well with saltation hop lengths on smooth beds after accounting for reductions in critical Shields stress.
Rough bed saltation hop lengths originally compiled by Sklar and Dietrich (2004); data sources include Abbott and Francis (1977), Lee and Hsu (1994), Nino et al. (1994), and Hu and Hui (1996a, b).

all other variables held constant) is caused by (i) lower energy particle-bed impacts associated with smaller w_s, and (ii) less frequent particle-bed impacts because of longer saltation-hop lengths for finer sediment moving at a higher transport stage.

The experimental observation that saltation hop length increases with transport stage (Fig. 7) leads to a counter-intuitive prediction in the saltation–abrasion model that beyond a threshold size, larger floods or steeper reaches produce lower erosion rates. For the case of sediment in suspension, the saltation–abrasion model assumes particles have infinite hop lengths and forces erosion rates to go to zero. Evaluating these predictions has been difficult, in part because, unlike saltation (Fig. 7), few data exist on particle impact rates at high transport stages with suspended sediment. Within the suspension-regime (i.e., $Z < 2.4$; Eq. (7)) saltation trajectories no longer follow ballistic paths but can be lofted high into the water column (Fig. 3) and travel distances $>10^2$–10^3 particle diameters between impacts (e.g., Francis, 1973; Nino et al., 2003). While individual particle motions within the suspension-regime are difficult to describe, the bulk sediment behavior is well described by active interchange between a near-bed layer where sediment may roll, slide, and saltate (i.e., the bedload) and a dilute layer above where motion is controlled by turbulence (i.e., the suspended load) (e.g., Rouse, 1937; McLean, 1991, 1992) (Fig. 3).

To account for the change in sediment transport mechanics between the bedload regime (i.e., $Z > 2.4$) and the suspension regime ($Z < 2.4$), Lamb et al. (2008b) recast the saltation–abrasion model in terms of near-bed sediment concentration rather than individual particle hop lengths. The Lamb et al. (2008b) model (hereafter referred to as the total-load model) predicts that erosion rates can increase for $Z < 2.4$ because of faster impact velocities associated with particles suspended within turbulent eddies that impinge on the bedrock, which increase the total impact rate and the volume of rock removed per impact. Scheingross et al. (2014) performed abrasion mill experiments focusing specifically on abrasion within the suspension regime. They measured finite erosion for grains as small as $D = 0.4$ mm ($Z = 0.8$), well within the suspension-regime, and observed suspended sediment transport with active particle-bed impacts and sediment concentrations increasing toward the bed, in agreement with suspension theory (e.g., Rouse, 1937; McLean, 1992) and previous experimental observations (e.g., Garcia and Parker, 1993). Erosion rates decreased with decreasing grain size, similar to the Sklar and Dietrich (2001) results, caused by the reduction in particle mass for small grain sizes, the lofting of a portion of the suspended load above the bedload layer (effectively decreasing the near-bed sediment concentration), and viscous dampening for fine sediment sizes (Fig. 6). The total-load model provides good agreement with the abrasion mill data of Sklar and Dietrich (2001) and Scheingross et al. (2014) in the bedload and in the suspension regimes when impacts are viscously damped for St < 75 (Eq. (8); Fig. 6).

3.3. Implications for zero-dimensional abrasion laws for field scale and comparison to stream power

The experiments of Sklar and Dietrich (2001) and Scheingross et al. (2014) were aimed at isolating and exploring key variables, such as transport stage in conjunction with sediment size, in existing bedrock-abrasion theory. In natural rivers, however, bed material size within a given reach is relatively constant, and instead changes in transport stage typically occur through changing water discharge and bed shear stress associated with floods. Analog experiments of floods are difficult to perform in zero-dimensional abrasion mills because of complications with secondary circulation that occurs under high shear stresses. Therefore, the total-load model is useful to explore scenarios more realistic for natural rivers.

Analysis of the total-load model shows that erosion rates can vary by orders of magnitude for the same transport stage (and therefore, the same particle trajectory), depending on the relative grain size, flow

depth, channel slope, and sediment supply (Fig. 8). Using base conditions representative of the South Fork Eel River reference site (Sklar and Dietrich, 2004), Scheingross et al. (2014) explored total-load model predictions by varying transport stages by changing either grain size, flow depth, or bed slope, while holding all other variables constant. This was performed for the case of constant sediment supply, q_s (as in the abrasion mills), and for sediment supply proportional to transport capacity, q_{sc} (as is more likely the case in bedrock rivers where extensive bed-cover is common; e.g., Johnson et al., 2009; DiBiase and Whipple, 2011). As was observed in abrasion mill experiments, when transport stage is varied by changing grain diameter, erosion rates decrease with increasing transport stage (τ^*/τ_c^*) owing predominately to the fine grain sizes that produce lower energy impacts (Fig. 8). For the case of constant sediment supply, increasing transport stage by increasing bed slope produces an initial decrease in erosion rate due to a lofting of a portion of the sediment above the bedload layer and increased particle velocities, both of which reduce the particle–bedrock impact rate. However, the increase in particle impact velocity associated with higher shear stress offsets the reduction in impact rate such that for high τ^*/τ_c^* erosion rates increase with τ^*/τ_c^*. If sediment supply is allowed to vary with transport capacity, as is often the case in natural rivers, the total-load model predicts that erosion rates continually increase with τ^*/τ_c^*, similar to stream power model predictions (Eq. (1)). For this case, higher sediment supply and faster impact velocities offset reductions in impact rate associated with particle trajectories. Thus, suspension-regime erosion creates a negative feedback in the development of knickpoints, whereby as channels steepen, erosion rates increase on the knickpoint surface relative to the lower-sloping channel segments above and below. This acts to reduce the knickpoint slope and also allows the knickpoint to continue upstream propagation. In contrast, bedload only erosion models predict that knickpoints stall out and can grow infinite in height when slopes become large enough for sediment to enter the suspension regime (Wobus et al., 2006; Crosby et al., 2007; Gasparini et al., 2007; Sklar and Dietrich, 2008).

In addition to the issues with abrasion mills in testing abrasion theories for the effects of large floods and steep bed slopes (Fig. 8), the representation of a river in the abrasion-mill as essentially zero-dimensional is a major limitation. Coarse sediment transport capacity (which is determined by depth, width, slope, and roughness together) does not evolve in the experiments but is instead imposed. Thus the effects of spatial variability of erosion within the channel as well as deposition of sediment, which together modify hydraulic geometry and roughness, are not addressed in these experiments, nor are they addressed in the saltation or total-load abrasion theories. The influence of particle trajectories and particularly the role of suspended sediment may be especially pronounced in channels with complex topography where suspended sediment can abrade objects protruding above the bedload layer. Limited experiments and theory have begun to address these factors as discussed in the next section.

4. Feedbacks among abrasion, bed roughness, and channel morphology

Several experiments have attempted to explore experimentally the coevolution of channel form and abrasion in bedrock channels in order to build on the understanding gained from abrasion mill experiments (Fig. 9; Table 1). Below we first highlight insight gained from experiments on the role of roughness in influencing bedrock incision, as well as feedbacks between incision and roughness. Next we highlight experimental evidence for the controls on channel width in bedrock channels, as well as its importance to the process of incision.

4.1. Effect of bedrock roughness on abrasion rate

Roughness is important to incision by abrasion because it influences the efficiency of sediment transport and the tendency for particles to be deposited on the bed. Because the abrasion rate averaged over the bed is strongly controlled by the extent of alluvial cover (Fig. 5), the growth of roughness on the bed may be a key mechanism that modulates the relationship between channel abrasion and sediment supply. Specifically, roughening of the channel increases the probability that mobile sediment grains will come to rest where they are shielded from the flow (e.g., Kirchner et al., 1990; Buffington and Montgomery, 1999; Chatanantavet et al., 2013). In addition, roughness will locally increase the friction angle for stationary grains on the bed, thereby increasing grain resistance to motion (e.g., Kirchner et al., 1990). Lastly, channel roughness can increase the form drag on conveyed fluid, thereby resulting in the progressive reduction in shear stress available for bedload transport (e.g., Manga and Kirchner, 2000).

Chatanantavet and Parker (2008) explored the relationships among sediment supply, sediment transport capacity, roughness, and alluvial deposition in a series of experiments using three different fixed

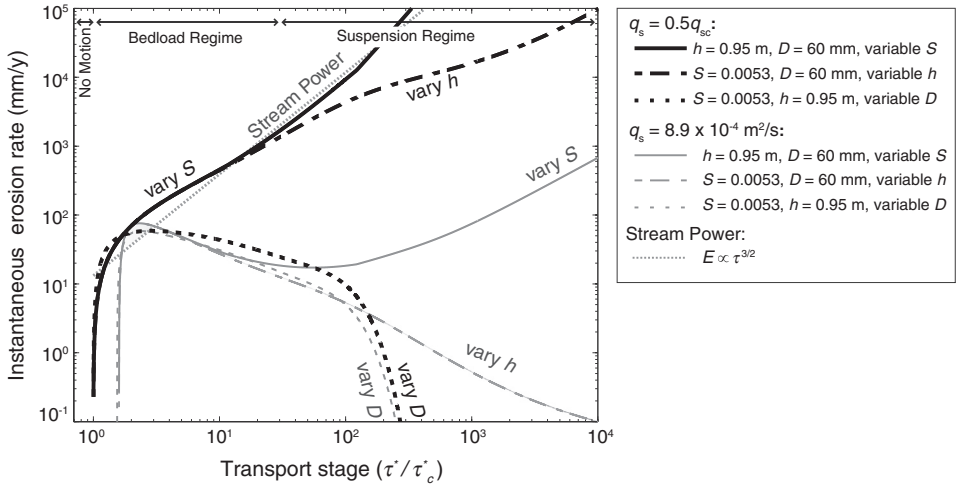

Fig. 8. Erosion rate predicted with total-load model for transport stage (τ^*/τ_c^*) varied by changing either grain size (D), channel slope (S), or flow depth (h), while holding all other values constant, for constant sediment supply (q_s; gray lines) and sediment supply proportional to transport capacity (q_{sc}; black lines) as predicted by Fernandez Luque and van Beek (1976). Also shown is the erosion rate predicted by stream power. All parameter values are representative of the South Fork Eel River, CA, USA, reference site (Sklar and Dietrich, 2004). The formulation $E \propto \tau^a$, where a is a constant commonly assumed equal to ~1.5, can be converted to the more familiar form of $E \propto A^m S^n$ (Eq. (1)) by assuming steady, uniform flow and combining a flow resistance relationship with empirical relationships relating channel width and water discharge to drainage area (e.g., Whipple et al., 2013).

Please cite this article as: Lamb, M.P., et al., New insights into the mechanics of fluvial bedrock erosion through flume experiments and theory, Geomorphology (2015), http://dx.doi.org/10.1016/j.geomorph.2015.03.003

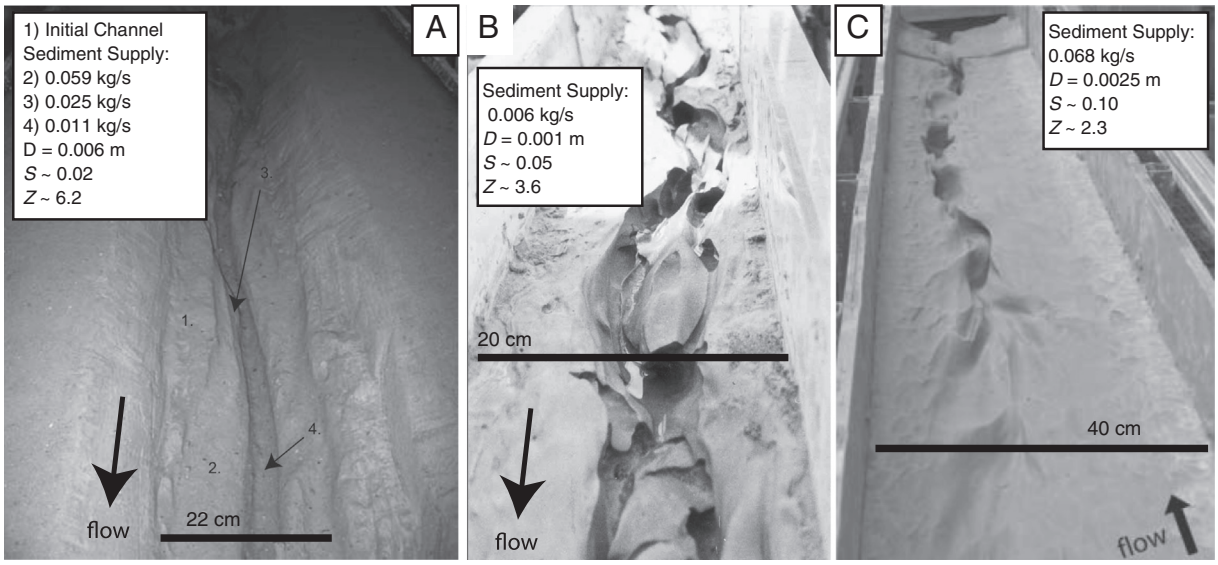

Fig. 9. Emergent channel morphologies evolved under increasing transport stage (τ^*/τ_c^*) from left (A) to right (C). The increase in channel tortuosity may reflect the evolution of these channels away from a saltation dominated channel toward a suspension-dominated channel.
Images are taken from (A) Finnegan et al. (2007) which evolved under three stages of decreasing sediment supply from an initial channel denoted by "1.", (B) Wohl and Ikeda (1997), and (C) Johnson and Whipple (2010).

roughness bedrock-bed morphologies (Table 1). A key observation of this experiment was a path dependence for bedrock channel alluviation. Smooth bedrock beds (defined as bed hydraulic roughness less than the composite grain and bar hydraulic roughness) developed stable partial alluvial cover if the initial condition was an alluvial bed. In contrast, a channel under the same boundary conditions, but with an initially sediment-free bed, would evolve to a completely alluviated state. This runaway alluviation process was also documented in flume experiments by Demeter et al. (2005) and Finnegan et al. (2007) (Table 1).

Chatanantavet and Parker (2008) argued that the runaway process occurs when bedrock hydraulic roughness is lower than the composite grain/bar hydraulic roughness in the alluviated state. Thus sediment deposition on a smooth bedrock bed is a positive feedback process in which deposited sediment creates more roughness and thus encourages more deposition, which in turn creates more roughness. In an experiment in which a 300-m-long, 0.8-m-deep channel was carved into weak bedrock in the field, Inoue et al. (2014) observed that the critical Shields stress of particles was typical of alluvial channels only when the ratio of bedrock hydraulic roughness was comparable to grain roughness. Otherwise, for bedrock channels that were hydraulically smoother than the alluviated bed, the critical Shields stresses were lower (0.01–0.02) than what is typically observed in alluvial channels. This observation supports Chatanantavet and Parker's (2008) argument in that it suggests that roughness because of deposited grains extracts more momentum from the flow than that associated with smooth, bare bedrock. Nelson and Seminara (2012), Inoue et al. (2014), and Johnson (2014) all presented theories that explain these observations by postulating differing grain and bedrock hydraulic roughnesses. A key prediction of these theories is that the nature of the transition from a bare bedrock to an alluvial state is controlled by the ratio of grain roughness to bedrock roughness. As inferred by Chatanantavet and Parker (2008), runaway alluviation occurs only when the grain hydraulic roughness is larger than the bedrock hydraulic roughness. When grain hydraulic roughness is comparable or smaller than bedrock hydraulic roughness, channels transition gradually from a bedrock to an alluvial state (Nelson and Seminara, 2012; Inoue et al., 2014; Johnson, 2014), a finding supported by the observation that a prealluviated bed did not experience runaway deposition in Chatanantavet and Parker's (2008) experiments. In addition, the theoretical findings of Nelson and Seminara (2012), Inoue et al. (2014), and Johnson (2014) are reinforced by the fact that roughness from artificial boulders in Chatanantavet and Parker's (2008) experiments supported stable partial alluvial cover.

In a set of experiments that explored the specific relationship between bedrock roughness and alluvial cover extent, Davis (2013) (Table 1) demonstrated essentially the same key result of Chatanantavet and Parker (2008), namely that partial alluvial cover can be supported when bed roughness is comparable to grain roughness. In addition, Davis (2013) and Johnson and Whipple (2010) (Table 1) showed that within the partial cover regime, the extent of alluvial cover on a bedrock bed for a

Table 1
Experimental parameters from bedrock incision experiments focused on the interaction of abrasion, roughness, sediment deposition, and channel form.

Study	Fr	Re	Flow velocity (m/s)	Flow depth (m)	Slope	Flume length (m)	Flume width (m)	Substrate	Sediment diameter (m)
Wohl and Ikeda (1997)	1.1–1.6	9000–93,500	0.5–1.1	0.015–0.085	0.01–0.2	4	0.2	70% fine sand, 30% bentonite	0.001
Finnegan et al. (2007)	1.2–1.4	120,000–140,000	1.2–1.4	0.1	0.02	6	0.3	Cement, fine sand, fly ash, flow additive	0.006
Johnson and Whipple (2007)	1.3–2.5	60,000–171,000	1.2–1.9	0.05–0.09	0.02–0.1	5	0.4	15:1 sand & Portland cement	0.0025
Chatanantavet and Parker (2008)	0.86–2.4	23,450–122,400	0.67–1.53	0.035–0.08	0.0115–0.03	13	0.9	Sand, cement, vermiculite	0.002 & 0.007
Johnson and Whipple (2010)[a]	2.4–3.5	6000–96,000	0.3–0.8	0.02–0.12	0.065	4	0.3	15:1 sand & Portland cement	0.0027–0.0055
Davis (2013) & Demeter et al. (2005)	0.68–1.26	70,000–82,000	0.75–1.12	0.08–0.13	0.0056–0.0073	6	0.3	10:1 fine sand & Portland cement	0.005

[a] Back-calculated flow velocity from reported Froude number and flow depth.

Please cite this article as: Lamb, M.P., et al., New insights into the mechanics of fluvial bedrock erosion through flume experiments and theory, Geomorphology (2015), http://dx.doi.org/10.1016/j.geomorph.2015.03.003

given sediment supply is linearly related to the amount of bed roughness (Fig. 10), as measured via the standard deviation of the detrended bed topography (as opposed to hydraulic roughness). These experimental results are also consistent with the theory of Nelson and Seminara (2012), Inoue et al. (2014), and Johnson (2014): if grain roughness is smaller than bedrock roughness, then deposition will smooth the bed, leading to an increase in transport efficiency with increasing deposition. The rougher a bedrock bed is, the more deposition needs to occur to smooth it to transport the imposed load. Thus, for a given supply rate, rougher beds support more alluvial cover than smoother beds, as observed in Davis (2013) and Johnson and Whipple (2010).

The observations in Davis (2013) and Johnson and Whipple (2010) demonstrated that bed roughness strongly modulates the relationship between channel abrasion rate and sediment supply through its influence on the efficiency of bedload transport and the deposition of alluvial sediment. Indeed, they show that roughness growth during incision is as important a control on alluvial cover as the supply of sediment itself. A key question that emerges from these experiments, then, is what actually determines roughness in natural bedrock channels? Is it determined by the process of abrasion, is it a property of the bedrock, or is it controlled by the alluvium that is deposited in the channel?

Several experiments have shed light on the processes governing the growth of bed roughness during abrasion of a bedrock channel. Using a flume with an erodible, preroughened concrete bed, Demeter et al. (2005) (Table 1) observed that at high sediment supply rates, topographic highs were preferentially eroded because low points were buried in gravel. A similar result was obtained by Finnegan et al. (2007) and Johnson and Whipple (2010). In these latter two examples, bedload transport on an initially smooth bed led to the cutting of a narrow slot (Fig. 9). Drag caused by the growth of this slot in both experiments ultimately led to deposition of a protective layer of alluvial cover on the bed, which in turn caused preferential erosion of the channel walls where they contacted the deposited gravel. Like Demeter et al. (2005), these experiments showed that partial alluvial cover focuses incision on exposed high points and thereby suppresses (Finnegan et al., 2007) or even reverses (Johnson and Whipple, 2010) the growth of roughness because of bedrock abrasion.

In contrast to cases with high sediment supply rates, Wohl and Ikeda (1997) (Table 1), Johnson and Whipple (2007, 2010), Finnegan et al. (2007), and Demeter et al. (2005) all showed that at low sediment supply rates relative to transport capacity, topographic low points were free of deposition and hence captured bedload and eroded more rapidly than neighboring high points, thereby cutting slots into the bedrock and increasing channel roughness. Wohl and Ikeda's (1997) experiments showed that the morphology of the emergent channel roughness depends strongly on channel slope. In particular, with increasing slope, slots become more tortuous (Fig. 9B). A reasonable hypothesis to explain this emergent pattern is that it reflects the change in erosional mechanics that occur as particles begin to transition from the saltation to the suspension regime (Fig. 3). As particles become entrained in the flow, abrasion is more strongly coupled to local turbulent flow structures. Thus emergent channel morphologies should depend on the Rouse number. Indeed, in Fig. 9 the two similarly tortuous channels (B, C) have Rouse numbers ($Z \sim 2.3$–3.6) that put them very close to the suspension threshold ($Z < 2.4$). Alternatively, Fig. 9A shows a much smoother and straighter channel with a Rouse number ($Z \sim 6.2$) that is well within the bedload regime ($Z > 2.4$).

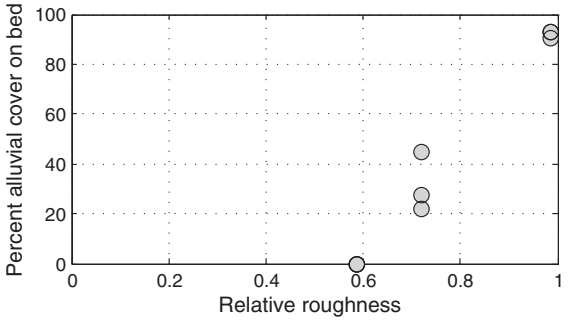

Fig. 10. Alluvial cover extent as a function of relative bed roughness from Davis (2013). Relative roughness is the standard deviation of residual bedrock-bed topography normalized by the grain diameter.

It is worth emphasizing that even for channels developed close to the suspension threshold (e.g., Wohl and Ikeda, 1997; Johnson and Whipple, 2007) the growth of bed roughness during slot cutting decreased the efficiency of sediment transport and did eventually trigger deposition of alluvial cover either locally or over the entire bed, thus returning the channel to a cover-limited regime in which roughness growth was suppressed or reversed. In addition, even in the absence of significant alluvial cover, isolated roughness elements that protrude into the flow may focus bedload abrasion. Several experiments demonstrate that the front side of protruding objects can be eroded and streamlined by sediment within the bedload regime (Johnson and Whipple, 2010; Wilson et al., 2013; Wilson and Lavé, 2014). Similarly, recent modification to the saltation–abrasion model by Huda and Small (2014) predicts enhanced erosion on the front side of protruding obstacles compared to that expected for a flat bed because of less oblique impacts on protruding obstacles resulting in higher energy impacts. Similar effects may also occur where sediment is suspended, and preliminary experiments show sediment in suspension preferentially erodes the upstream side of protruding objects (Cornell, 2007).

Taken together, the experiments described above hint at the possibility that the presence or absence of significant alluvial cover on a bedrock river bed may control whether roughness increases or decreases on a bedrock bed. Smooth bedrock beds lead to the growth of roughness through slot cutting (Demeter et al., 2005; Finnegan et al., 2007; Johnson and Whipple, 2010). Rough beds, because they encourage coarse sediment deposition in channel low points, preferentially erode exposed highs and reduce roughness (Demeter et al., 2005; Finnegan et al., 2007; Johnson and Whipple, 2010). Thus feedbacks between abrasion, roughness growth, and sediment deposition clearly exist and point to a key future research question. Can a stable bed roughness, alluvial cover extent, and abrasion rate emerge for a given sediment supply? Or is the process of abrasion fundamentally unstable?

4.2. Lateral abrasion rates, vertical incision, and channel width

The width of a channel is important to river incision into bedrock because it determines the bed area over which sediment can be transported and influences the magnitude and spatial variation of fluid stresses applied to the bed. However, the controls on channel width and its relationship to both sediment transport and incision in bedrock channels remain poorly understood. Bedrock channel width adjustment can occur by widening caused by lateral wear of channel walls and narrowing because of focused incision over only part of the channel cross section. Thus, the variability in the spatial distribution of incision directly influences the extent and rate of channel width adjustment.

Five experiments have addressed the controls on width adjustment in bedrock channels undergoing abrasion (Wohl and Ikeda, 1997; Carter and Anderson, 2006; Finnegan et al., 2007; Johnson and Whipple, 2010; Fuller, 2014). In these experiments, roughness (through its influence on sediment transport and deposition) and sediment supply (through its influence on the width over which active incision occurs) represent potentially key controls on width evolution.

Wohl and Ikeda (1997), Finnegan et al. (2007), and Johnson and Whipple (2010) all documented the growth of abrasional inner channels on the floor of initially flat flumes (Fig. 9). Finnegan et al. (2007) and Johnson and Whipple (2010) observed that when their experimental channels were free of alluvial cover on the bed, incision was focused

Please cite this article as: Lamb, M.P., et al., New insights into the mechanics of fluvial bedrock erosion through flume experiments and theory, Geomorphology (2015), http://dx.doi.org/10.1016/j.geomorph.2015.03.003

over a fraction of the bed width that varied strongly with bedload supply. For a fixed-slope channel with a smooth bed, narrow slots were carved for low sediment supply rates and wider slots were carved for higher supply rates. This change in slot width can be seen in Fig. 9A, where remnants of channels evolved under different sediment supplies are visible. Both experiments discussed above observed an approximately linear increase in slot width with sediment supply, suggesting that the zone of active bedload transport and hence of active incision into bedrock varies as a function of bedload supply. The scaling of abrasional channel width with sediment supply is explained in a theoretical analysis by Nelson and Seminara (2011). Bedload moves downstream at a characteristic velocity for a given shear stress (e.g., Sklar and Dietrich, 2004). To accommodate an imposed sediment supply for a given stress, only the width over which active bedload transport occurs can adjust. Hence abrasion width and bedload supply are linked.

In both experiments of Finnegan et al. (2007) and Johnson and Whipple (2010), the growth of roughness because of slot cutting eventually led to the deposition of alluvial cover on the bed. This, in turn, led to concentrated transport and incision on the edges of the alluvial deposit and thereby encouraged channel widening. Thus, the results of these experiments indicate that channels can adjust their width by changing the region over which vertical incision takes place in the channel. Moreover, because the pattern of incision on the bed in these experiments is controlled by sediment supply and sediment deposition, the results of these experiments suggest that width, like roughness, may evolve in response to changes in sediment supply or transport capacity. That said, integrating all of the magnitude and frequency variation in sediment supply and water flux experienced by a typical river is a key challenge in connecting the experimental morphologies to natural channels.

Fuller (2014) addressed the role of roughness in governing lateral abrasion more directly. In this experiment, bed roughness was varied systematically along the length of a synthetic bedrock bed by changing the size of particles fixed to the bed. Rates and patterns of lateral wear were then documented using a scanning laser. The key result of this experiment was that above a critical roughness value, rough sections of the channel exhibited rates of lateral wear that were 3–5 times higher than adjacent smooth channel sections (Fig. 11). Fuller hypothesized that this dramatic difference in lateral wear reflects the fact that rougher beds deflect particles away from the downstream transport direction and into the channel walls more effectively than smooth beds.

Erosion by suspended sediment may also exert a key influence on bedrock channel width. Suspended sediment lofted into the water column can erode channel sidewalls above the bedload layer height, and erosion of sidewalls by suspended sediment can occur even if the bed is partially or fully covered with sediment (Hartshorn et al., 2002). Widening of sidewalls from suspension–regime erosion likely occurred in the flume experiments on slot-canyon evolution by Carter and Anderson (2006), for example.

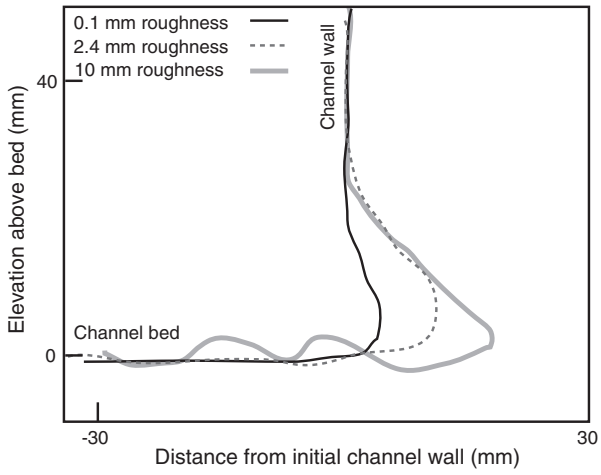

Fig. 11. Patterns of wall abrasion from Fuller (2014) for a single sediment supply rate with variable channel roughness. Higher lateral erosion rates associated with larger bed roughness shift the channel profile to the right.

5. Erosion by plucking

In addition to abrasion, plucking is recognized as an important mechanism in fluvial bedrock erosion (e.g., Miller, 1991; Annandale, 1995; Whipple et al., 2000), although it has received considerably less study experimentally. Here we review theory and limited experiments for erosion rates by plucking in Section 5.1; derive new thresholds for plucking by vertical entrainment, sliding, and toppling in Section 5.2; and assess the relative roles of entrainment versus transport in setting the rate of plucking in Section 5.3.

5.1. Erosion rate

In the only complete theoretical model for fluvial erosion by plucking to date, Chatanantavet and Parker (2009) envision, through the process of exhumation, intact rock moving vertically first through an *aging layer*, where rock fractures because of erosional unloading and chemical weathering, and second through a *battering layer* where fracturing progresses through impacts caused by saltating sediment (similar to the process of abrasion discussed in Section 4) until block sizes are sufficiently small to be removed hydraulically. In Chatanantavet and Parker (2009), the entrainment rate (E) follows a form well known for the entrainment of loose bed sediment into transport:

$$\frac{E}{\left(RgD_p\right)^{1/2}} = a_p\left(\tau^* - \tau_{pc}^*\right)^{n_p} \tag{14}$$

where $R = (\rho_r - \rho_w)/\rho_w$ is the submerged specific density of sediment, D_p is the characteristic block size, τ_{pc}^* is the threshold value of Shields stress to initiation plucking, and a_p and n_p are empirical coefficients. Tsujimoto (1999), for example, indicate $a_p = 0.0199$, $n_p = 1.5$, and $\tau_{pc}^* = 0.045$ for loose sediment, values adopted by Chatanantavet and Parker for plucking. Chatanantavet and Parker (2009) also include factors in Eq. (14) to account for the availability of pluckable chunks on the bed because of cover by alluvium or incomplete aging and battering. Similar to experimentally verified models for alluvial cover discussed in Section 4 (e.g., Fig. 5), alluvial cover is parameterized as a linear function of the sediment supply relative to sediment transport capacity of bedload sediment:

$$\frac{q_{sc}}{\left(RgD^3\right)^{1/2}} = a_s\left(\tau^* - \tau_c^*\right)^{n_s} \tag{15}$$

in which a_s and n_s are empirical coefficients. Fernandez Luque and van Beek (1976), for example, suggested $a_s = 5.7$ and $n_s = 1.5$.

Few tests of the plucking theory exist, and moreover it is not known whether rock fracture, entrainment of blocks, or the downstream transport of blocks is the rate limiting step in fluvial erosion by plucking (Howard et al., 1994). As discussed by Howard (1998) and Whipple et al. (2000), the prevalence of alluvium in rivers cutting through jointed rocks suggests that entrainment and transport are often the rate limiting mechanisms. The lack of observations in natural rivers is in part because erosion by plucking occurs during infrequent, extreme events. One rare test of the transport-limited idea comes from the formation of Canyon Lake Gorge, TX, USA, a natural experiment in which lake spillover in 2001 created an ~15-m-deep gorge in well-jointed limestone in a matter of days. Lamb and Fonstad (2010) showed that formation of the gorge is consistent with a model in which the erosion rate is limited by the transport of the blocks, similar to

Please cite this article as: Lamb, M.P., et al., New insights into the mechanics of fluvial bedrock erosion through flume experiments and theory, Geomorphology (2015), http://dx.doi.org/10.1016/j.geomorph.2015.03.003

Eq. (14). Similarly, Chatanantavet and Parker (2011) found good agreement between their model (Chatanantavet and Parker, 2009) and observations of knickpoint retreat by block plucking in a small plucking-dominated stream in Indiana, USA (Miller, 1991).

The only experimental test of the rate of rock erosion by plucking, to our knowledge, is the work of Dubinski and Wohl (2013) who cast abrasion-resistant, sand–cement mixtures into rectangular blocks creating a bedrock bed with joints parallel and perpendicular to the bed surface (Fig. 12). Although a few blocks were plucked through vertical entrainment, most erosion occurred through block sliding at a knickpoint face (where blocks lacked a downstream neighbor). Dubinski and Wohl (2013) found that the erosion rate followed expectations from bedload transport and entrainment relationships similar to Eq. (15) and was consistent with limited field observations (e.g., Lamb and Fonstad, 2010; Chatanantavet and Parker, 2011). These results suggest that the rate of plucking erosion via block sliding at a knickpoint may also be well represented by Eq. (14) even though the process of block sliding is not explicitly included in the model.

5.2. Threshold for block entrainment

Although the threshold for sediment entrainment in rivers has been studied extensively in experiments for nearly a century (Shields, 1936; Brownlie, 1983; Wilcock, 1993; Prancevic et al., 2014), comparatively little work has been done on the threshold for block entrainment in bedrock river beds (see Carling and Tinkler (1998) for a review). Three mechanisms that are typically considered for block removal (e.g., George and Sitar, 2012) are: (i) vertical entrainment leaving behind a hole, (ii) downstream block sliding where the downstream neighbor has already been removed, and (iii) downstream toppling of a block where the downstream neighbor has already been removed. Determining the controls on these thresholds is important for predicting incision rates by plucking (e.g., Eq. 14).

5.2.1. Vertical entrainment

For vertical entrainment, Hancock et al. (1998) considered the critical stress for entrainment by balancing hydraulic lift with submerged block weight and argued that block height (H, Fig. 13) is the sole dimension of importance for resistance of block movement because of gravity. Whipple et al. (2000) added frictional stresses along the block sides to the theory for vertical entrainment and showed that, in addition to larger block heights, blocks with smaller lengths in the downstream direction (L, Fig. 13) and widths in the cross-stream direction (W) relative to block height should be more resistant to erosion. Experimental tests to date have largely neglected frictional wall stresses and instead focused on the important role of in-crack pressure fluctuations (e.g., USBR, 2007) and protrusion of the block above the surrounding river bed. For example, Reinius (1986) measured pressure around test blocks rotated at various angles relative to the river flow and found block protrusion to be significant in inducing forces that entrain blocks. Coleman et al. (2003) performed systematic experiments on vertical entrainment of prismatic blocks with little sidewall friction and found that the threshold stress for block entrainment depends linearly on the submerged block weight per unit bed area and inversely on the block protrusion height (P, Fig. 13) normalized by the block length. Coleman et al. (2003) cast their experimental results in terms of a critical Shields stress for plucking as:

$$\tau^*_{pc} = 0.0015\left(\frac{P}{L}\right)^{-1} + 0.002 \tag{16}$$

Fig. 12. Blocks eroded primarily by sliding (top) at a waterfall face from Dubinski and Wohl (2013) looking upstream (left) and in planview (right). Toppling of blocks (bottom) before (left) and after (right) failure at a waterfall from Lamb and Dietrich (2009).

Please cite this article as: Lamb, M.P., et al., New insights into the mechanics of fluvial bedrock erosion through flume experiments and theory, Geomorphology (2015), http://dx.doi.org/10.1016/j.geomorph.2015.03.003

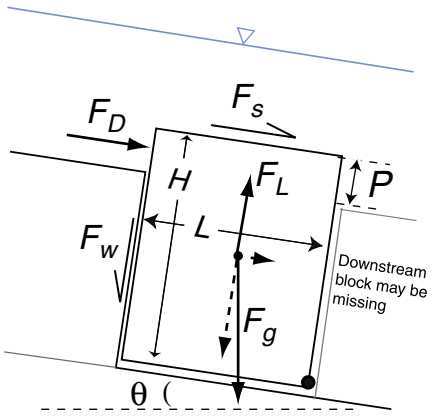

Fig. 13. Forces and dimensions considered for plucking of a block of height H and length L by vertical entrainment, sliding or toppling from a bed inclined at angle θ. For sliding and toppling the downstream block is assumed to be missing and for toppling the torque balance is about the pivot point at the bottom right corner of the block (filled circle). Forces considered include buoyancy and gravity (F_g), bed shear stress (F_s), form drag associated with protrusion of the block (F_D) by amount P, hydraulic lift (F_L), and frictional forces along the block side walls (F_w). Not shown are the block width (W), frictional stress along the base of the block when sliding, and frictional wall stresses along the page-parallel planes.

where

$$\tau_{pc}^{*} \equiv \frac{\tau_b}{(\rho_r - \rho_w)gH}. \tag{17}$$

Eq. (16) has been subsequently verified in additional flume experiments for the vertical entrainment of prismatic blocks (Melville et al., 2006); however, as noted by Melville et al. (2006) an exponential decay function may be more appropriate as τ_{pc}^{*} should not tend to infinity for the limiting case of $P = 0$.

To synthesize the existing theory and experimental work on vertical entrainment of blocks and the relative roles of block side friction, protrusion, and block dimensions, here we propose a new derivation for vertical entrainment building on the force balance model of Whipple et al. (2000) but cast in terms of a critical Shields stress, following the work of Wiberg and Smith (1987) for entrainment of sediment. In subsequent sections we will also derive new relationships for the threshold of sliding and toppling that will aid in comparison of the relative role of the three mechanisms and highlight where experimental tests are needed.

For river flow over the top of a well-jointed, fully submerged, rectangular block with river-bed parallel and perpendicular joint sets, we consider the combined forces of buoyancy and gravity (F_g), downstream-directed bed shear stress (F_s) and form drag associated with protrusion of the block (F_D), hydraulic lift directed perpendicular to the bed surface (F_L), and frictional forces along the block side walls (F_w) (Fig. 13), as:

$$F_g = LWHg(\rho_r - \rho_w) \tag{18.1}$$

$$F_s = \tau_b LW \tag{18.2}$$

$$F_D = 0.5\rho_w C_D u^2 PW \tag{18.3}$$

$$F_L = F_L^{*}(F_D + F_s) \tag{18.4}$$

$$F_w = \tau_w A_w \tag{18.5}$$

where C_D is a local drag coefficient, u is the downstream flow velocity acting on the protruded part of the block, and τ_w is the frictional stress along the block sidewalls acting over an area A_w. We parameterize the lift force as a linear function of the combined forces due to drag and shear. Wiberg and Smith (1987) suggest that the empirical constant $F_L^{*} = 0.85$; however, this coefficient has considerable variability (Schmeeckle et al., 2007).

To solve for the threshold for vertical entrainment, and assuming the river bed gradient is at an angle of θ (Fig. 13), we set equal the destabilizing force of lift to the stabilizing forces of gravity and frictional forces along the walls as,

$$F_L = F_g\cos\theta + F_w = F_g\cos\theta + 2\tau_w H(L + W) \tag{19}$$

which assumes that the frictional stresses are equal on all four sides of the block and the protrusion height is small compared to the block height ($P \ll H$). Substituting Eqs. (18.1), (18.2), (18.3), (18.4) and (18.5) into Eq. (19) and rearranging results in

$$\tau_{pc}^{*} = \frac{\tau_b}{(\rho_r - \rho_w)gH} = \frac{\left(\cos\theta + 2\tau_w^{*}\left(1 + \frac{W}{L}\right)\right)}{F_L^{*}\left(1 + \frac{1}{2}C_D\left(\frac{u}{u_*}\right)^2\frac{P}{L}\right)} \tag{20}$$

in which $\tau_w^{*} = \frac{\tau_w}{(\rho_r - \rho)gW}$ is a dimensionless block sidewall stress.

Eq. (20) allows for scaling between field and laboratory conditions for plucking by explicitly including the parameters that depend on fluid viscosity and the effect of river and block scale through the particle Reynolds number (Eq. (6)) dependence of C_D and the flow Reynolds number dependence of $\frac{u}{u_*}$ (Eq. (4)), as discussed in Section 2.1 (e.g., Schlichting, 1979). For example, C_D varies with particle Reynolds number for small particle Reynolds numbers but is approximately constant ($C_D \sim 1$; e.g., Schlichting, 1979; Schmeeckle et al., 2007) for $Re_p > 100$, conditions typical of most natural rivers, allowing direct comparison to flume experiments that also have $Re_p > 100$. Likewise, because we are interested in the velocity near the height of the protruding block ($z = P$), and assuming that bed roughness is similar to the block protrusion height ($k_s = P$), Eq. (4) reduces to a constant $u(z = P)/u_* = 8.3$ for fully turbulent and hydraulically rough flow. Eq. (20) matches the experimental data of Coleman et al. (2003) well (Fig. 14A). Data scatter at low τ_{pc}^{*} corresponds to cases with large protrusion heights relative to block heights (e.g., $P/H > 0.5$), which is unlikely in natural rivers and also violates our assumption of $P \ll H$ in the derivation of Eq. (20).

Eq. (20) also is consistent with previous work in that the block height (H) emerges as the dominant length scale in the resistive force per unit area due to particle weight (e.g., Hancock et al., 1998) and that the protrusion height relative to block length, rather than block height alone, is crucial in determining the threshold for entrainment (Coleman et al., 2003). The denominator of the right-hand side (rhs) of Eq. (20) contains two terms: the first of which is unity, and the second term contains block protrusion height. Because $C_D \sim 1$ and $(u(z = P)/u_*)^2 \approx 8.3^2 = 69$ for turbulent, hydraulically rough flow, the protrusion height need only be a small fraction (greater than a few percent) of the block length to have a significant effect on block entrainment (Fig. 14B). This rationale is consistent with existing experiments that show a strong effect of P/L on vertical entrainment (Coleman et al., 2003; Melville et al., 2006) (Eq. (16)). Coleman et al. (2003) noted that their results for τ_{pc}^{*} were significantly lower than expected by comparison of transport thresholds for sediment (e.g., $\tau_c^{*} = 0.045$; Fig. 14A), and they speculated this may be a particle-shape effect as they investigated rectangular blocks rather than rounded particles. However, according to Eq. (20), particle-shape effects would need to manifest in more than an order of magnitude increase in drag (C_D) for blocks relative to gravel to explain the data, which is unlikely based on drag-coefficient studies (e.g., Schlichting, 1979; Schmeeckle et al., 2007). Instead, we propose that the comparatively low values of τ_{pc}^{*} observed by Coleman et al. (2003) were because of their smooth perspex bed upstream of the

Please cite this article as: Lamb, M.P., et al., New insights into the mechanics of fluvial bedrock erosion through flume experiments and theory, Geomorphology (2015), http://dx.doi.org/10.1016/j.geomorph.2015.03.003

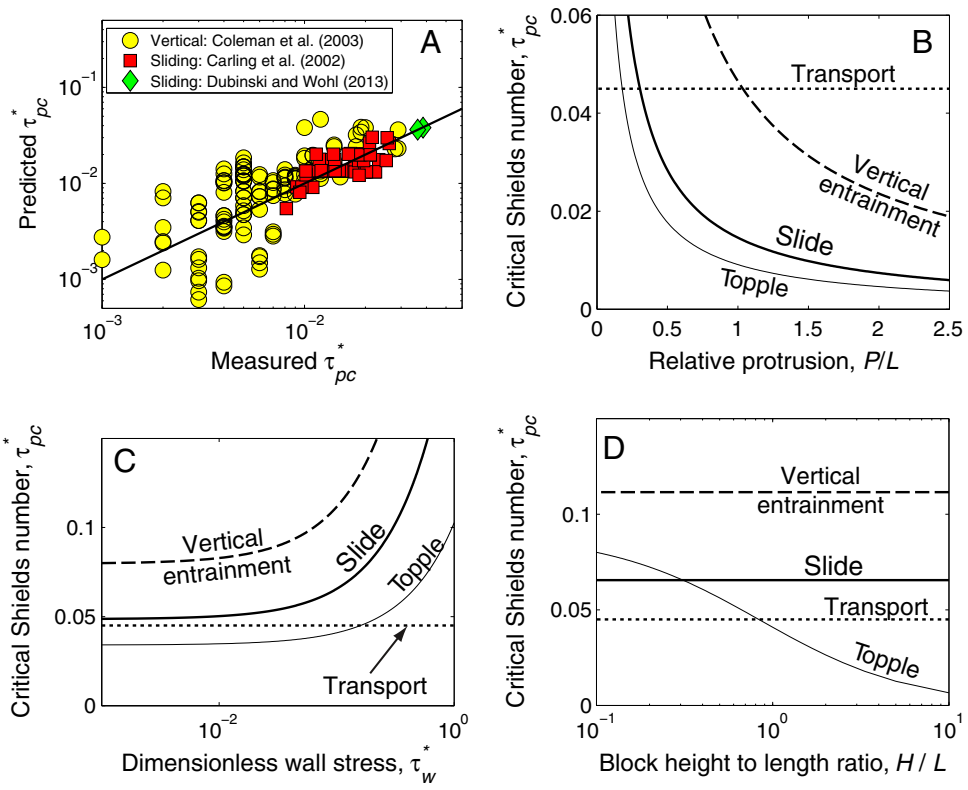

Fig. 14. Critical Shields stress for plucking through vertical entrainment (Eq. (20)), sliding (Eq. (22)) and toppling (Eq. (24)), and the critical Shields stress for incipient sediment transport. (A) Model predictions for sliding (Eq. (22)) and vertical entrainment (Eq. (20)) versus measured critical Shields numbers calculated from the experimental data of Carling et al. (2002), Coleman et al. (2003), and Dubinski and Wohl (2013). The solid line represents a one-to-one correspondence. For these cases u/u_* was calculated using the log law and bed roughness values from the experiments (1.5 mm for Carling et al. (2002), hydraulically smooth for Coleman et al. (2003) and hydraulically rough for Dubinski and Wohl (2013)). We assume wall stresses are zero ($\tau^*_w = 0$) in Coleman et al. (2003) owing to the smooth blocks. Carling et al. (2002) used isolated blocks resting on a planar bed, thus $P = H$ and $\tau^*_w = 0$ for those experiments. The remaining panels show model predictions versus (B) relative block protrusion (P/L), (C) dimensionless block wall friction ($\tau^*_w = \tau_w/[(\rho_r - \rho_w)gW]$), and (D) relative block height (H/L) with all other parameters held constant at $C_D = 1$, $F^*_L = 0.85$, $\tan\theta = 0.007$, $\phi = 30°$, $\tau^*_w = 0.1$, $W/L = 1$, $H/L = 1$, and $P/L = 0.2$. Panels (B)–(D) assume $u(z = P)/u_* = 8.3$ corresponding to hydraulically rough, turbulent flow where the bed roughness length is equal to P, conditions that are likely in natural rivers.

blocks of interest, which resulted in a hydraulically smooth flow and near-bed flow velocities that were increased substantially compared to the hydraulically rough case. Our model results are consistent with data of Coleman et al. (2003) using $u(z = P)/u_* = 20$ (Fig. 14A), which corresponds to the case of hydraulically smooth flow for the bed-shear stresses observed in their experiments.

Overall, the model result for vertical entrainment for a hydraulically rough bed suggest that entrainment becomes increasingly difficult for $P/L < 0.5$, which is likely for many natural rivers (Fig. 14B). For the case of $P = 0$, τ^*_{pc} for vertical entrainment approaches unity, similar to criteria for incipient suspension (Eq. (7)), which is highly unlikely for large blocks unless the river is experiencing a very extreme flood event.

Eq. (20) suggests that larger block widths (W) reduce the role of wall stresses in resisting entrainment (Whipple et al., 2000). As expected, the data of Coleman et al. (2003) show no effect of block width because they had smooth, low-friction block sidewalls. The numerator of the rhs of Eq. (22) shows two terms, the first of which is $\cos\theta$ that is near unity for most rivers (Fig. 13). This suggests that τ^*_w must also be of order unity to play a significant role in resisting block entrainment (Fig. 14C). Dimensionless wall stress of $\tau^*_w \approx 1$ implies that sidewall stresses must be approximately equivalent to the block weight per unit area. Such large wall stresses are probably unlikely unless significant interlocking or cohesive bonds exist between blocks. This rationale may explain why experiments have yet to find a significant effect of wall stress, or block width and length, on entrainment thresholds (Coleman et al., 2003; Dubinski and Wohl, 2013). Experiments with significant interlocking have yet to be performed, however, and τ^*_w provides a dimensionless scale parameter to compare interlocking and frictional stresses along block walls between experimental and field cases.

5.2.2. Sliding

Dubinski and Wohl (2013) observed that the main process of erosion in their experiments was not vertical entrainment but downstream sliding of blocks at a vertical-step knickpoint (which in their case was also a waterfall) (Fig. 12). This is consistent with the experimental results of Carling et al. (2002) for their cases with isolated, fully submerged blocks. Hancock et al. (1998) derived a formula for the threshold of block sliding by considering the forces of fluid or bed shear stress and submerged block weight. Following Whipple et al. (2000), Dubinski and Wohl (2013) modified the formulation of Hancock et al. (1998) to include friction along the block sides, and the revised theory showed that smaller block width adds to stability whereas smaller block lengths may decrease stability. Despite including wall stresses (and therefore the role of block width and length) into the theory, the experimental results of Dubinski and Wohl for the threshold of sliding using concrete blocks showed nearly equivalent entrainment stresses of 16 and 17 Pa despite a factor of two increase in block width and length (i.e., a factor of four increase in block weight) for blocks of $W = L = 3$ and 6 cm (all with $H = 3$ cm). Using Eq. (20), these results are nearly equivalent, and $\tau^*_{pc} = 0.036$ and 0.039 for their small and large blocks, respectively, and are counter to the theory of Whipple et al. (2000) that the critical stress for sliding should decrease with increasing block width and length.

Here we derive a critical Shields stress for block sliding following the assumptions and formulations used above for vertical block entrainment. Importantly, we assume that blocks are well submerged in the flow (e.g., see Carling et al. (2002) for the role of block emergence) and that there is not a waterfall at the free face (see Section 6 for a separate discussion on bedrock erosion by waterfalls). We consider a

force balance parallel to the bed in which the upstream-directed force that resists motion from bed friction follows a Mohr–coulomb friction relationship (e.g., Wiberg and Smith, 1987),

$$F_g \sin\theta + F_s + F_D = \left(F_g \cos\theta - F_L\right)\tan\phi + F_w \tag{21}$$

in which $(F_g \cos\theta - F_L)$ represents the bed-normal force and tan ϕ is a bed friction angle. For the case of sliding, the wall stress acts only on two walls of the block (parallel to the flow direction), so that $F_w = 2\tau_w LH$. Substituting these expressions into Eqs. (17) and (21) and rearranging results in

$$\tau^*_{pc} = \frac{\tau_b}{(\rho_r - \rho_w)gH} = \frac{\cos\theta(\tan\phi - \tan\theta) + 2\tau^*_w}{\left(1 + \frac{1}{2}C_D\left(\frac{u}{u_*}\right)^2\frac{P}{L}\right)(1 + F^*_L\tan\phi)}. \tag{22}$$

Typical values of friction angles between slabs of rock range from about $\phi = 20°$ to 45° (Selby, 1993; Carling and Tinkler, 1998).

Our sliding model (Eq. (22)) matches well the experimental data of Dubinski and Wohl (2013) and Carling et al. (2002) for block sliding (Fig. 14A). The experiments of Carling et al. (2002) are for initial motion of isolated, centimeter-scale, prismatic blocks (i.e., $\tau^*_w = 0$) of various dimensions that slid across a planar, rough bed (i.e., $P = H$) with bed roughness lengths of 1 to 2 mm (Fig. 14A). Like the threshold model for vertical entrainment, inspection of Eq. (22) shows again that τ^*_w must be order unity (i.e., frictional wall stresses must be a significant portion of the block weight per unit sidewall area) in order for wall stresses or block width to be important in limiting sliding (Fig. 14C). Wall friction is less important for sliding, as compared to vertical entrainment, caused by reduction in wall-contact area (four frictional boundaries versus two). In contrast to wall friction, bottom friction and block protrusion (or lack thereof) likely dominate the resistance to sliding in well-jointed rock (Fig. 14B), consistent with experimental results that show virtually no effect of block width on erosion thresholds (Carling et al., 2002; Dubinski and Wohl, 2013). As expected, the threshold for sliding is always significantly less than the threshold for vertical entrainment (Fig. 14), indicating that block sliding at steps in the river bed likely dominates over vertical entrainment in natural rivers, at least in bedrock with near river-bed-parallel joints.

5.2.3. Toppling

Lamb and Dietrich (2009) argued that blocks without a downstream neighbor (Fig. 13) are more likely to topple than to slide if $H/L > 0.5$ and formulated a stability model for block toppling as a function of torques due to gravity, buoyancy, bed shear stress and drag associated with protrusion of the top of the block into the flow. Their specific application was for toppling of blocks at the face of waterfalls, and they found good agreement between model and measurement in a flume experiment using stacked blocks with large H/L (Fig. 12). This is consistent with the experiments of Dubinski and Wohl (2013) in that they also observed block toppling more often for their case of $H/L = 1$ (small blocks) in comparison to $H/L = 0.5$ (large blocks) (I. Dubinski, Colorado State University, personal communication, 2014). In addition, Carling et al. (2002) demonstrated that toppling may dominate over sliding for isolated blocks that are partially emergent from the flow. Here we extend the torque-balance model of Lamb and Dietrich (2009) to the case of toppling of blocks at a bedrock step that is well submerged (i.e., no waterfall) and cast it in terms of a critical Shields stress to make comparisons between the theories derived above for vertical entrainment and sliding. To our knowledge, no experiments have been conducted on toppling of fully submerged blocks.

We balance the torques due to shear, drag, and lift across the top of the column and gravity (if the column is leaning downstream) against the resisting torques of gravity and frictional forces against the column walls (Fig. 13):

$$\frac{1}{2}H\sin\theta F_g + H(F_s + F_D) + \frac{1}{2}L\cos\theta F_L = \frac{1}{2}L\cos\theta\left(F_g + F_w\right). \tag{23}$$

In this case, like the sliding block, the frictional forces along the two sidewalls of the block are given by $F_w = 2\tau_w LH$. Rearranging Eq. (23) in terms of a critical Shields stress results in

$$\tau^*_{pc} = \frac{\tau_b}{(\rho_r - \rho_w)gH} = \frac{\frac{L}{H}\cos\theta\left[\frac{1}{2}\left(1 - \frac{H}{L}\tan\theta\right) + \tau^*_w\right]}{\left(1 + \frac{1}{2}C_D\left(\frac{u}{u_*}\right)^2\frac{P}{L}\right)\left(1 + \frac{1}{2}F^*_L\frac{L}{H}\cos\theta\right)}. \tag{24}$$

Like the previous theories for vertical entrainment and sliding, similar parameters emerge in the toppling threshold including dimensionless wall stress (τ^*_w, which again is unlikely to be important unless it is order unity) and block protrusion height normalized by block length (P/L) (Fig. 14B and C). Most importantly for toppling, however, is the dominant role of block height normalized by length (H/L), which dramatically lowers stability for tall and skinny columns (Fig. 14D), consistent with the experimental results of Lamb and Dietrich (2009) (Fig. 12). Inspection of Eq. (24) shows that for toppling, in contrast to vertical entrainment and sliding, the dominant length scale that determines the stabilizing stress due to block weight is the downstream block length (L) rather than the block height (H). This result occurs because an increase in block height increases the block weight (which linearly adds stability) and increases the torque arm associated with drag and shear forces across the block top (which linearly decreases stability), such that results are only weakly sensitive to block height alone (except where block tilt angles are large). In contrast, block height to length ratio (H/L) has a strong effect on the threshold for toppling, whereas it has no (independent) effect on the thresholds for vertical entrainment or sliding (Fig. 14D). Consequently, block toppling is expected to dominate over sliding and vertical entrainment at bedrock steps for $H/L >$ ~0.5 to 1.

5.3. Entrainment versus transport-limited erosion

There are no experimental or field tests of the relative roles of block entrainment versus downstream sediment transport (sensu Howard et al., 1994) in setting the rate of bedrock erosion by plucking. Assuming that the rate of rock fracture is not the rate-limiting mechanism (e.g., Howard, 1998; Whipple et al., 2000), Eqs. (14) and (15) can be combined to evaluate the relative roles of entrainment and sediment transport in setting the erosion rate. Specifically, using mass balance and assuming a constant channel width, we can solve for the characteristic length scale (l_E), herein referred to as an adaption length, over which the capacity of the flow to transport entrained blocks (i.e., q_{sc}) in an initially clearwater flow becomes the rate-limiting step to further entrainment, as

$$l_E \equiv \frac{q_{sc}}{E} = 285D\left(\frac{\tau^* - \tau^*_c}{\tau^* - \tau^*_{pc}}\right)^{1.5} \tag{25}$$

where $n_p = n_s = 1.5$ and $a_s/a_p = 285$ following the values reported above, and the characteristic block diameter is assumed to be equivalent to the characteristic sediment size ($D_p = D$). Under the special case where the threshold for plucking blocks is the same threshold as for transport (i.e., $\tau^*_{pc} = \tau^*_c$), then Eq. (25) reduces to a linear function of

Please cite this article as: Lamb, M.P., et al., New insights into the mechanics of fluvial bedrock erosion through flume experiments and theory, Geomorphology (2015), http://dx.doi.org/10.1016/j.geomorph.2015.03.003

block size:

$$l_E = 285D. \quad (26)$$

Eq. (26) suggests, for example, that if the typical block diameter is $D = 1$ m, then sediment transport will set the erosion rate for any reach longer than $l_E = 285$ m (assuming spatially uniform τ^* within the reach). Block entrainment is the rate limiting factor only for reach length smaller than 285 m — and potentially over much smaller length scales depending on the sediment supply to the reach from upstream and from the neighboring hillsides. However, if the threshold for block entrainment is larger than that for sediment transport (i.e., $\tau^*_{pc} > \tau^*_c$), then l_E given by Eq. (25) can be significantly larger than $285D$ signifying an increased role of block entrainment in limiting erosion. For example, Fig. 15 shows the solutions to Eq. (25) for different transport stages (i.e., τ^*/τ^*_c), in which a value of τ^*/τ^*_c of 1.2 is common for gravel-bed rivers for reference (e.g., Parker et al., 2007). As the ratio of the plucking threshold relative to the sediment transport threshold (i.e., τ^*_{pc}/τ^*_c) approaches the transport stage, then l_E grows infinitely large, indicating the dominance of block entrainment over sediment transport in setting the erosion rate. Fig. 15 also shows that erosion during extreme floods ($\tau^*/\tau^*_c \gg 1$) is more likely to be transport-limited as l_E is small, unless the threshold for entrainment is much larger than the threshold for transport. In contrast, for more regular floods ($\tau^*/\tau^*_c \sim 1.2$), subtle differences between the threshold to entrain blocks and the threshold for transport dictate whether erosion by plucking is entrainment or transport limited, and therefore likely depends on whether plucking is due to vertical entrainment, sliding or toppling.

Entrainment thresholds for plucking are highly sensitive to block protrusion length relative to block length (Fig. 14B), with large relative protrusion tending toward transport-limited conditions, and zero protrusion tending toward entrainment-limited erosion rates. Wall stresses that approach the block weight per unit area also significantly limit block entrainment (Fig. 14C) and erosion rates shift toward a transport-limited state. If rivers are limited to plucking by vertical entrainment alone, entrainment rates are likely be the rate-limiting step to bedrock erosion even with negligible wall friction. However, erosion is more likely to be concentrated at bedrock steps that promote sliding and toppling because the erosion thresholds for these processes are typically far lower than the threshold for vertical block entrainment (Fig. 14). This may explain the prevalence of stepped (rather than holey) topography in plucking-dominated landscapes and signifies the important role of knickpoint retreat in landscapes with well-jointed rock (e.g., Miller, 1991; Weissel and Seidl, 1997; Mackey et al., 2014). Thresholds for block sliding are similar to sediment transport, such that the limiting factors on erosion rates where sliding is dominant may vary from place to place depending largely on the block friction angle (ϕ). Plucking rates in the sliding-dominated Canyon Lake Gorge, TX, for example, appear to have been set by the rate of sediment transport (Lamb and Fonstad, 2010). Finally, at a bedrock step where $H/L > 1$, toppling is likely to dominate over sliding, and toppling thresholds are typically far less than the threshold for transport indicating the likely scenario of transport-limited erosion rates in these landscapes (Fig. 14D), consistent with field observations in canyons cut into columnar basalt (Lamb et al., 2008a, 2014).

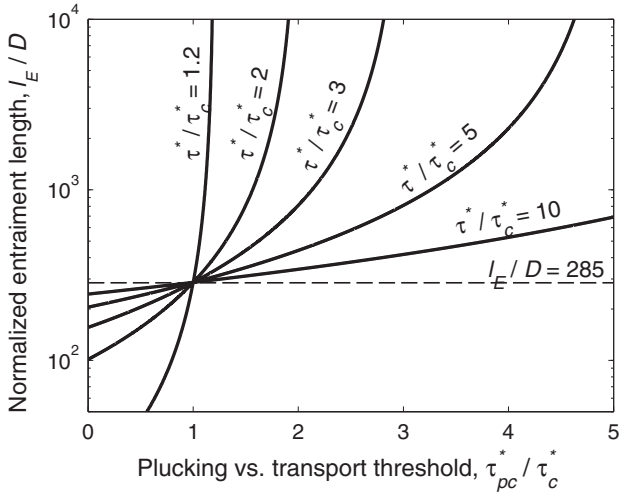

Fig. 15. Normalized adaption length beyond which entrainment rates by plucking in an initially clearwater flow becomes transport limited (Eq. (25)) as a function of the critical Shields stress for plucking normalized by that for sediment transport (τ^*_{pc}/τ^*_c). Solid contours show different flood events with different transport stages (τ^*/τ^*_c). The dashed line is the solution to Eq. (25) for the case of $\tau^*_{pc}/\tau^*_c = 1$. For this figure, the characteristic block diameter is assumed to be equivalent to the characteristic sediment size ($D_p = D$).

6. Abrasion and plucking at waterfalls

At a steep drop in the river bed, water may detach from the bedrock face forming a waterfall and plunge-pool. Erosion at waterfalls is important to understand because waterfalls can be the fastest eroding parts of some landscapes, and they can communicate changes in tectonics, climate, and sea-level throughout a drainage basin (e.g., Gilbert, 1907; Howard et al., 1994; DiBiase et al., 2014; Mackey et al., 2014). Some workers have applied saltation–abrasion theories to steep river reaches and waterfalls (e.g., Chatanantavet and Parker, 2006; Wobus et al., 2006; Crosby et al., 2007; Gasparini et al., 2007; Goode and Burbank, 2009); however, these theories are unlikely to hold for high gradient rivers. Beyond a certain river-channel slope of approximately 10%, approximations (e.g., shallow water approximation) and empirical formulations for hydraulics and sediment transport discussed for abrasion and plucking become increasingly invalid (e.g., Yager et al., 2007; Lamb et al., 2008c). For example, the bedload-only saltation abrasion model shows a decrease in erosion rates with increasing channel bed slope, but limited experimental data indicate the opposite trend (Wohl and Ikeda, 1997; Johnson and Whipple, 2007). As another example, theory (Parker and Izumi, 2000) and experiments show that steep river beds rapidly evolve into a series of cyclic steps (or bedrock step pools) for clearwater flows over cohesive beds (Brooks, 2001) and for sediment-transporting flows over concrete beds (Yokokawa et al., 2013) because of strong morphodynamic feedbacks that do not occur for low-gradient bedrock rivers. At the extreme case of a waterfall, even the assumption of hydrostatic pressure is no longer valid (Rouse, 1936). Consequently, new theories and experiments are needed that explicitly address abrasion and plucking erosion processes in steep rivers and at waterfalls.

Most experiments on waterfall erosion to date have focused on waterfall formation and retreat following base-level drop. Gardner (1983) performed experiments in homogeneous cohesive sediments, where rapid erosion of vertical waterfall faces led to decreased waterfall slopes and the eventual replacement of waterfalls with steepened reaches extending across the majority of the flume length. Experiments in stratified sediments of alternating strength show different behaviors. Holland and Pickup (1976) and Frankel et al. (2007) observed that vertical waterfalls tend to form on locally resistant layers and that undercutting of the weaker layer via plunge-pool erosion allows the waterfall to keep its form during retreat, similar to investigations of gully headcut erosion (e.g., Bennett et al., 2000) and the classic model of Gilbert (1907). Such experiments have led to models of waterfall retreat via failure of a cantilever caprock (e.g., Stein and LaTray, 2002; Haviv et al., 2010; Hayakawa and Matsukura, 2010); however, these models lack an explicit process-based treatment of plunge-pool bedrock abrasion and plucking. Wells et al. (2010) demonstrated that upstream sediment supply can slow plunge-pool erosion and headcut retreat in soil.

Lamb et al. (2007) modified the saltation–abrasion model for waterfall plunge-pool erosion by accounting for the kinetic energy of particle-impacts as sediment accelerates over a waterfall and decelerates

Please cite this article as: Lamb, M.P., et al., New insights into the mechanics of fluvial bedrock erosion through flume experiments and theory, Geomorphology (2015), http://dx.doi.org/10.1016/j.geomorph.2015.03.003

through a water-filled plunge pool. In their model, predictions of vertical plunge-pool erosion depend critically on the sediment transport capacity of the plunge pool, $q_{sc\text{-}pool}$, as vertical incision requires the plunge pool floor to be cover-free. While experiments of clearwater overspilling onto loose sediment have shown $q_{sc\text{-}pool}$ scales with shear stress at the base of the pool (e.g., Stein et al., 1993; Stein and Julien, 1994), it is unclear if this formulation should hold for bedrock plunge pools where steep sidewalls require sediment to be suspended out of the pool. Only one experiment exists that investigates plunge-pool erosion by abrasion using a sand–cement mixture (Iguchi and Sekiguchi, 2008), but these results have yet to be compared to theory.

In contrast to bedrock abrasion at waterfall plunge pools, a wealth of experiments have been performed on the plucking of jointed rock by high velocity jets within plunge pools due to the application to concrete dams and spillways (e.g., Annandale, 1995). Experiments by Robinson et al. (2001) showed that threshold for plucking of rectangular concrete blocks by a waterfall jet agrees well with a simple force balance model (Hanson et al., 1998) in which blocks are plucked when the force associated with the stagnation pressure of the impinging jet overcomes the combined weight of the block and overlying column of water. Other models relate pressure fluctuations to the plucking of blocks (e.g., Bollaert, 2004), and numerous experimental studies have explored how pressure fluctuations on the plunge-pool floor vary with plunge-pool geometry, jet air entrainment, joint spacing, and more (e.g., Ervine et al., 1997; Bollaert and Schleiss, 2003; Manso et al., 2009). Little work has been done to extend this engineering-oriented work to natural waterfalls or to explore experimentally the long-term geomorphic implications of plucking in knickpoint retreat.

In addition to erosion within a waterfall plunge-pool, the brink of the waterfall escarpment may also erode. In this scenario, the fluvial erosion theories discussed in Sections 3 and 4 for abrasion and plucking can be adapted for flow acceleration and loss of hydrostatic pressure at the waterfall lip (e.g., Stein and Julien, 1994; Haviv et al., 2006). For the cases of block sliding and toppling, Dubinski and Wohl (2013) and Lamb and Dietrich (2009) also considered the potential lack of hydrostatic pressure at the downstream face of the block and the degree of submergence within a plunge pool, finding good agreement between experiments and theory.

7. Some future opportunities

Although laboratory experiments have contributed greatly to our understanding of bedrock channel processes, tremendous opportunities remain for future experiments. Here we briefly suggest fruitful directions for experimentation, focusing in particular on the detachment mechanisms of abrasion and plucking.

A key next step in understanding abrasion of bedrock by mobile sediments is to explore the effect of nonuniform sediment size distributions. Previous experiments have maintained narrow size distributions, but natural bedrock channels are supplied with and thus transport sediment mixtures containing a wide range of particle sizes. As the grain size distribution widens, particle interactions will influence the threshold and stability of transient alluvial deposits responsible for the cover effect. Size selective deposition and mobilization may affect the size distribution in transport for a given shear stress. Experiments that explore mixed sediment sizes in laboratory bedrock channels may need to be combined with experiments investigating the effect of variable discharge and the partially-decoupled nature of discharge and sediment supply. A rich parameter space encompassing distributions of discharge, sediment supply, and grain size remains to be explored.

Future experiments are also needed to further explore the role of bedload and suspended sediment on erosion in complex topography and at high transport stages. Mixed sediment size distributions supplied to erodible laboratory channels with significant bed roughness may result in spatial partitioning of incision mechanisms, with suspended sediments acting on elevated surfaces and bedload restricted to lower portions of the channel. Bed roughness is likely to evolve because of feedbacks between the relative mobility and spatial sorting of sediments. A related set of questions concerns wear of channel banks and evolution of cross section morphology. Abrasion by particle impacts may be an effective mechanism for channel widening and lateral migration, but perhaps only if channels have significant planform sinuosity and fluctuations in sediment supply limit vertical incision. An important consideration will be scaling morphodynamics for channel evolution in addition to producing hydraulics in laboratory channels with sufficient turbulence to drive suspended sediments against banks at velocities that overcome the viscous damping of impacts.

Surprisingly few experiments have been conducted on erosion rate by plucking and the entrainment of blocks by fluvial processes. No experiments to our knowledge have investigated fracturing and weathering processes to create jointed rock, nor the interactions between rock fracturing, bedload saltation, and abrasion. Also missing is an exploration of feedbacks between erosion rates and channel morphology in a plucking-dominated river, although initial progress has been made for the special case of plucking at waterfalls (Lamb and Dietrich, 2009; Dubinski and Wohl, 2013).

Other morphodynamic topics ripe for experimental investigation include channel response to transient base-level fall, plunge-pool erosion below waterfalls, and the formation of strath terraces by alternating episodes of lateral and vertical incision. Detachment mechanisms other than abrasion and plucking also deserve experimental attention, including the potential for cavitation and segregation ice growth to influence rock erosion when conditions are favorable.

8. Conclusions

Laboratory experiments are opening the door to quantitative testing of fluvial bedrock erosion models in ways that are difficult or impossible to perform in natural rivers. Equally important, exploratory experiments yield much needed insight into the evolving interactions between river-channel form, hydraulics, and sediment transport — dynamics that typically unfold over thousands of years or longer in nature. A significant milestone in bedrock erosion experiments is the discovery that rock erodibility by abrasion, across substrates including concrete, foam, ice, and a variety of bedrock lithologies, is a function of rock tensile strength, which allows erosion laws calibrated in the laboratory to be readily scaled for natural rivers on Earth and other planets and moons. In addition to rock tensile strength, erodibility experiments suggest that rock resistance to abrasion is better represented by fracture toughness rather than elasticity, and we propose a new representation of abrasion theory that can incorporate fracture toughness, which motivates future experiments.

In addition to rock strength, abrasion experiments have revealed the dominant and nonlinear role of sediment, including sediment size, transport mode, particle trajectories, and sediment supply, in setting erosion rates. The frontier of bedrock-erosion experiments includes unraveling the morphodynamic feedbacks between hydraulics, channel roughness, sediment transport, and evolving channel morphology. Specifically, roughness, through its influence on the patterns of sediment deposition and through its influence on saltation trajectories, exerts a strong control on channel width, a long-standing fundamental unknown in geomorphology.

Revised and unified theory for the threshold for vertical entrainment, sliding and toppling of blocks, combined with limited experimental data, highlights the dominant role that knickpoints play in bedrock erosion by plucking. These theories also highlight key dimensionless parameters that can be used to scale plucking experiments to natural rivers. The combination of rate laws for plucking and sediment transport shows that block toppling is likely a transport-limited process, whereas vertical entrainment and in cases sliding may be detachment-limited. However, the competition between rate-limiting mechanisms also depends on the magnitude of flood events, in which large floods tend toward transport-limited conditions.

Please cite this article as: Lamb, M.P., et al., New insights into the mechanics of fluvial bedrock erosion through flume experiments and theory, Geomorphology (2015), http://dx.doi.org/10.1016/j.geomorph.2015.03.003

Observations from laboratory experiments continue to force the advancement of theory in fluvial bedrock erosion, which in turn exposes knowledge gaps in field observations and leads to new expectations in landscape evolution.

Author contributions

All authors contributed equally to this work.

Acknowledgments

With pleasure we thank Paul Carling, Sean Bennett, and Cheryl McKenna Neuman for formal reviews that strengthened the paper, Richard Marston for his detailed edits, and the conveners and scientific committee of the 46th Annual Binghamton Symposium for bringing this special issue to fruition. MPL and JSS thank Daniel Lo for helping in foam erosion rate calibration studies and Brian Fuller for bringing river experimentation back to life at Caltech. Ian Dubinski kindly shared photos and insight from his study. Paul Carling made available data from his block sliding experiments. This work was supported by NSF grant EAR-1147381 and NASA grant 12PGG120107 to MPL, and NSF grant EAR-0345344 to LSS. JSS was partially supported by an NSF Graduate Student Research Fellowship.

References

Abbott, J.E., Francis, J.R.D., 1977. Saltation and suspension trajectories of solid grains in a water stream. Philos. Trans. R. Soc. A Math. Phys. Eng. Sci. 284 (1321), 225–254. http://dx.doi.org/10.1098/rsta.1977.0009.

Annandale, G.W., 1995. Erodibility. J. Hydraul. Res. 33 (4), 471–494.

Bagnold, R.A., 1966. An approach to the sediment transport problem for general physics. US Geological Survey Professional Paper 422-I, Washington, D.C.

Baker, V.R., 1973. Paleohydrology and sedimentology of the Lake Missoula flooding in eastern Washington. Geol. Soc. Am. Spec. Pap. 144, 79.

Baker, V.R., Pickup, G., 1987. Flood geomorphology of the Katherine-Gorge, Northern-Territory, Australia. Geol. Soc. Am. Bull. 98 (6), 635–646. http://dx.doi.org/10.1130/0016-7606(1987)98<635:fgotkg>2.0.co;2.

Bennett, S.J., Alonso, C.V., Prasad, S.N., Romkens, M.J.M., 2000. Experiments on headcut growth and migration in concentrated flows typical of upland areas. Water Resour. Res. 36 (7), 1911–1922. http://dx.doi.org/10.1029/2000wr900067.

Beyeler, J.D., Sklar, L.S., 2010. Bedrock resistance to fluvial erosion: the importance of rock tensile strength, crystal grain size and porosity in scaling from the laboratory to the field. Eos Trans. AGU 91 (52) (Fall Suppl., Abstract EP41D-0740).

Bitter, J.G.A., 1963. A study of erosion phenomena: part I. Wear 6, 5–21.

Black, B.A., Perron, J.T., Burr, D.M., Drummond, S.A., 2012. Estimating erosional exhumation on Titan from drainage network morphology. J. Geophys. Res. Planets 117. http://dx.doi.org/10.1029/2012je004085.

Bollaert, E., 2004. A new and comprehensive model to evaluate scour formation in plunge pools. Hydropower Dams (1).

Bollaert, E., Schleiss, A., 2003. Scour of rock due to the impact of plunging high velocity jets part II: experimental results of dynamic pressures at pool bottoms and in one- and two-dimensional closed end rock joints. J. Hydraul. Res. 41 (5), 465–480.

Bonnet, S., Crave, A., 2003. Landscape response to climate change: insights from experimental modeling and implications for tectonic versus climatic uplift of topography. Geology 31 (2), 123–126. http://dx.doi.org/10.1130/0091-7613(2003)031<0123:lrtcci>2.0.co;2.

Bridges, N.T., Laity, J.E., Greeley, R., Phoreman, J., Eddlemon, E.E., 2004. Insights on rock abrasion and ventifact formation from laboratory and field analog studies with applications to Mars. Planet. Space Sci. 52 (1–3), 199–213. http://dx.doi.org/10.1016/j.pss.2003.08.026.

Brocard, G.Y., Van Der Beek, P.A., Bourlès, D.L., Siame, L.L., Mugnier, J.L., 2003. Long-term fluvial incision rates and postglacial river relaxation time in the French Western Alps from 10Be dating of alluvial terraces with assessment of inheritance, soil development and wind ablation effects. Earth Planet. Sci. Lett. 209 (1), 197–214.

Brocklehurst, S.H., Whipple, K.X., 2007. Response of glacial landscapes to spatial variations in rock uplift rate. J. Geophys. Res. Earth Surf. 112 (F2). http://dx.doi.org/10.1029/2006jf000667.

Brooks, P.C., 2001. Experimental Study of Erosional Cyclic Steps. (Masters). University of Minnesota, Minnesota.

Brownlie, W.R., 1983. Flow depth in sand-bed channels. J. Hydraul. Eng. ASCE 109 (7), 959–990.

Buffington, J.M., Montgomery, D.R., 1999. Effects of hydraulic roughness on surface textures of gravel-bed rivers. Water Resour. Res. 35 (11), 3507–3521. http://dx.doi.org/10.1029/1999WR900138.

Burr, D.M., Perron, J.T., Lamb, M.P., Irwin III, R.P., Collins, G.C., Howard, A.D., Sklar, L.S., Moore, J.M., Adamkovics, M., Baker, V.R., Drummond, S.A., Black, B.A., 2013. Fluvial features on Titan: insights from morphology and modeling. Geol. Soc. Am. Bull. 125 (3–4), 299–321. http://dx.doi.org/10.1130/b30612.1.

Carling, P., Tinkler, K., 1998. Conditions for the entrainment of cuboid boulders in bedrock streams: an historical review of literature with respect to recent investigations. In: Tinkler, K.J., Wohl, E.E. (Eds.), Rivers Over Rock: Fluvial Processes in Bedrock Channels. Geophysical Monograph 107. American Geophysical Union, Washington, D.C., pp. 19–33.

Carling, P.A., Hoffmann, M., Blatter, A.A., Dittrich, A., 2002. Drag of emergent and submerged rectangular obstacles in turbulent flow above bedrock surface. In: Schleiss, A.J., Bollaert, E. (Eds.), Rock Scour due to Falling High-velocity Jets. Swets and Zeitlinger, Lisse, pp. 83–94.

Carter, C.L., Anderson, R.S., 2006. Fluvial erosion of physically modeled abrasion-dominated slot canyons. Geomorphology 81 (1–2), 89–113. http://dx.doi.org/10.1016/j.geomorph.2006.04.006.

Chatanantavet, P., Lamb, M.P., 2014. Sediment transport and topographic evolution of a coupled river and river-plume system: an experimental and numerical study. J. Geophys. Res. Earth Surf. http://dx.doi.org/10.1002/2013JF002810.

Chatanantavet, P., Parker, G., 2006. Modeling the bedrock river evolution of western Kaua'i, Hawai'i, by a physically-based incision model based on abrasion. In: Parker, G., Garcia, M. (Eds.), River, Coastal and Estuarine Morphodynamics 2005. Taylor and Francis Group.

Chatanantavet, P., Parker, G., 2008. Experimental study of bedrock channel alluviation under varied sediment supply and hydraulic conditions. Water Resour. Res. 44 (12), W12446. http://dx.doi.org/10.1029/2007WR006581.

Chatanantavet, P., Parker, G., 2009. Physically based modeling of bedrock incision by abrasion, plucking, and macroabrasion. J. Geophys. Res. Earth Surf. 114. http://dx.doi.org/10.1029/2008jf001044.

Chatanantavet, P., Parker, G., 2011. Quantitative testing of model of bedrock channel incision by plucking and macroabrasion. J. Hydraul. Eng. ASCE 137 (11), 1311–1317. http://dx.doi.org/10.1061/(asce)hy.1943-7900.0000421.

Chatanantavet, P., Whipple, K.X., Adams, M.A., Lamb, M.P., 2013. Experimental study on coarse grain saltation dynamics in bedrock channels. J. Geophys. Res. Earth Surf. 118 (2), 1161–1176. http://dx.doi.org/10.1002/jgrf.20053.

Clarke, B.A., Burbank, D.W., 2010. Bedrock fracturing, threshold hillslopes, and limits to the magnitude of bedrock landslides. Earth Planet. Sci. Lett. 297 (3–4), 577–586. http://dx.doi.org/10.1016/j.epsl.2010.07.011.

Coleman, S.E., Melville, B.W., Gore, L., 2003. Fluvial entrainment of protruding fractured rock. J. Hydraul. Eng. ASCE 129 (11), 872–884. http://dx.doi.org/10.1061/(asce)0733-9429(2003)129:11(872).

Collins, G.C., 2005. Relative rates of fluvial bedrock incision on Titan and Earth. Geophys. Res. Lett. 32 (22). http://dx.doi.org/10.1029/2005gl024551.

Cook, K.L., Turowski, J.M., Hovius, N., 2013. A demonstration of the importance of bedload transport for fluvial bedrock erosion and knickpoint propagation. Earth Surf. Process. Landf. 38 (7), 683–695. http://dx.doi.org/10.1002/esp.3313.

Cornell, K.M., 2007. Suspended Sediment Erosion in Laboratory Flume Experiments. (Masters), Massachusetts Institute of Technology, Cambridge, MA (50 pp.).

Croissant, T., Braun, J., 2014. Constraining the stream power law: a novel approach combining a landscape evolution model and an inversion method. Earth Surf. Dyn. 2, 155–166. http://dx.doi.org/10.5194/esurf-2-155-2014.

Crosby, B.T., Whipple, K.X., Gasparini, N.M., Wobus, C.W., 2007. Formation of fluvial hanging valleys: theory and simulation. J. Geophys. Res. Earth Surf. 112 (F3). http://dx.doi.org/10.1029/2006jf000566.

Davis, J.R., 2013. The Influence of Bed Roughness on Partial Alluviation in Bedrock Channels. (MS). San Francisco State University, San Francisco, CA.

Demeter, G.I., Sklar, L.S., Davis, J.R., 2005. The influence of variable sediment supply and bed roughness on the spatial distribution of incision in a laboratory bedrock channel. Eos Trans. AGU 86 (52) (Abstract H53D-0519).

DiBiase, R.A., Whipple, K.X., 2011. The influence of erosion thresholds and runoff variability on the relationships among topography, climate, and erosion rate. J. Geophys. Res. Earth Surf. 116. http://dx.doi.org/10.1029/2011jf002095.

DiBiase, R.A., Whipple, K.X., Heimsath, A.M., Ouimet, W.B., 2010. Landscape form and millennial erosion rates in the San Gabriel Mountains, CA. Earth Planet. Sci. Lett. 289 (1–2), 134–144. http://dx.doi.org/10.1016/j.epsl.2009.10.036.

DiBiase, R.A., Whipple, K.X., Lamb, M.P., Heimsath, A.M., 2014. The role of waterfalls and knickzones in controlling the style and pace of landscape adjustment in the western San Gabriel Mountains, CA. Geol. Soc. Am. Bull. http://dx.doi.org/10.1130/B31113.1.

Dubinski, I.M., Wohl, E., 2013. Relationships between block quarrying, bed shear stress, and stream power: a physical model of block quarrying of a jointed bedrock channel. Geomorphology 180, 66–81. http://dx.doi.org/10.1016/j.geomorph.2012.09.007.

Dzulynski, S., Sanders, J.E., 1962. Current Marks on Firm Mud Bottoms, Transactions of the Connecticut Academy of Arts and Sciences. The Connecticut Academy of Arts and Sciences, New Haven, pp. 57–96.

Einstein, H.A., 1950. The bed-load function for sediment transportation in open channel flow. US Dept. Agric. Tech. Bull. 1026, 1–71.

Engle, P., 1978. Impact Wear of Materials. Elsevier Sci., New York.

Ervine, D.A., Falvey, H.T., Withers, W., 1997. Pressure fluctuations on plunge pool floors. J. Hydraul. Res. 35 (2), 257–279.

Fernandez Luque, R., van Beek, R., 1976. Erosion and transport of bed-load sediment. J. Hydraul. Res. 14, 127–144.

Ferrier, K.L., Huppert, K.L., Perron, J.T., 2013. Climatic control of bedrock river incision. Nature 496 (7444), 206–209. http://dx.doi.org/10.1038/nature11982.

Finnegan, N.J., Sklar, L.S., Fuller, T.K., 2007. Interplay of sediment supply, river incision, and channel morphology revealed by the transient evolution of an experimental bedrock channel. J. Geophys. Res. Earth Surf. 112 (F3). http://dx.doi.org/10.1029/2006jf000569.

Finnegan, N.J., Schumer, R., Finnegan, S., 2014. A signature of transience in bedrock river incision rates over time scales of 104–107 years. Nature 505, 391–394. http://dx.doi.org/10.1038/nature12913.

Please cite this article as: Lamb, M.P., et al., New insights into the mechanics of fluvial bedrock erosion through flume experiments and theory, Geomorphology (2015), http://dx.doi.org/10.1016/j.geomorph.2015.03.003

Francis, J.R.D., 1973. Experiments on motion of solitary grains along bed of a water-stream. Proc. R. Soc. Lond. A 332 (1591), 443–471. http://dx.doi.org/10.1098/rspa.1973.0037.
Frankel, K.L., Pazzaglia, F.J., Vaughn, J.D., 2007. Knickpoint evolution in a vertically bedded substrate, upstream-dipping terraces, and Atlantic slope bedrock channels. Geol. Soc. Am. Bull. 119 (3–4), 476–486. http://dx.doi.org/10.1130/b25965.1.
Fuller, T.K., 2014. Field, Experimental and Numerical Investigations Into the Mechanisms and Drivers of Lateral Erosion in Bedrock Channels. (PhD). University of Minnesota, Minneapolis, MN.
Ganti, V., Lamb, M.P., McElroy, B., 2014. Quantitative bounds on morphodynamics and implications for reading the sedimentary record. Nat. Commun. 5. http://dx.doi.org/10.1038/ncomms4298.
Garcia, M., Parker, G., 1993. Experiments on the entrainment of sediment into suspension by a dense bottom current. J. Geophys. Res. Oceans 98 (C3), 4793–4807. http://dx.doi.org/10.1029/92jc02404.
Gardner, T.W., 1983. Experimental study of knickpoint and longitudinal profile evolution in cohesive, homogeneous material. Geol. Soc. Am. Bull. 94 (5), 664–672. http://dx.doi.org/10.1130/0016-7606(1983)94<664:esokal>2.0.co;2.
Gasparini, N.M., Brandon, M.T., 2011. A generalized power law approximation for fluvial incision of bedrock channels. J. Geophys. Res. Earth Surf. 116. http://dx.doi.org/10.1029/2009jf001655.
Gasparini, N.M., Whipple, K.X., Bras, R.L., 2007. Predictions of steady state and transient landscape morphology using sediment-flux-dependent river incision models. J. Geophys. Res. Earth Surf. 112 (F3). http://dx.doi.org/10.1029/2006jf000567.
George, M., Sitar, N., 2012. Evaluation of Rock Scour Using Block Theory. ICSE6, Paris, pp. 1457–1464.
Gilbert, G.K., 1877. Report on the Geology of the Henry Mountains. Geographical and Geological Survey of the Rocky Mountain Region. Government Printing Office, Washington D.C. (106 pp.).
Gilbert, G.K., 1907. The rate of recession of Niagara Falls. US Geol. Surv. Bull. 306, 1–31.
Gilbert, G.K., 1914. The transportation of debris by running water. US Geological Survey Professional Paper 86. Government Printing Office, Washington D.C. (263 pp.).
Goode, J.K., Burbank, D.W., 2009. Numerical study of degradation of fluvial hanging valleys due to climate change. J. Geophys. Res. Earth Surf. 114. http://dx.doi.org/10.1029/2007jf000965.
Goudie, A.S., 2006. The Schmidt hammer in geomorphological research. Prog. Phys. Geogr. 30 (6), 703–718. http://dx.doi.org/10.1177/0309133306071954.
Grotzinger, J.P., Hayes, A.G., Lamb, M.P., McLennan, S.M., 2013. Sedimentary processes on Earth, Mars, Titan and Venus. In: Mackwell, S., Bullock, M., Harder, J. (Eds.), Comparative Climatology of Terrestrial Planets. University of Arizona Press, pp. 439–472.
Hancock, G.S., Anderson, R.S., Whipple, K.X., 1998. Beyond power: bedrock river incision process and form. In: Tinkler, K.J., Wohl, E.E. (Eds.), Rivers Over Rock: Fluvial Processes in Bedrock Channels. American Geophysical Union. Geophysical Monograph 107. American Geophysical Union, Washington, D.C., pp. 35–60.
Hancock, G.S., Small, E.E., Wobus, C., 2011. Modeling the effects of weathering on bedrock-floored channel geometry. J. Geophys. Res. 116, F03018. http://dx.doi.org/10.1029/2010JF001908.
Hanson, G.J., Robinson, K.M., Cook, K.R., 1998. Erosion of structured material due to impinging jet. Proceedings of the 1998 ASCE International Water Resources Engineering Conference, Memphis, Tenn, pp. 1102–1107.
Hartshorn, K., Hovius, N., Dade, W.B., Slingerland, R.L., 2002. Climate-driven bedrock incision in an active mountain belt. Science 297 (5589), 2036–2038. http://dx.doi.org/10.1126/science.1075078.
Hasbargen, L.E., Paola, C., 2000. Landscape instability in an experimental drainage basin. Geology 28 (12), 1067–1070. http://dx.doi.org/10.1130/0091-7613(2000)28<1067:liiaed>2.0.co;2.
Hatzor, Y.H., Palchik, V., 1997. The influence of grain size and porosity on crack initiation stress and critical flaw length in dolomites. Int. J. Rock Mech. Min. Sci. Geomech. Abstr. 34 (5), 805–816. http://dx.doi.org/10.1016/s1365-1609(96)00066-6.
Haviv, I., Enzel, Y., Whipple, K.X., Zilberman, E., Stone, J., Matmon, A., Fifield, L.K., 2006. Amplified erosion above waterfalls and oversteepened bedrock reaches. J. Geophys. Res. Earth Surf. 111 (F4). http://dx.doi.org/10.1029/2006jf000461.
Haviv, I., Enzel, Y., Whipple, K.X., Zilberman, E., Matmon, A., Stone, J., Fifield, K.L., 2010. Evolution of vertical knickpoints (waterfalls) with resistant caprock: insights from numerical modeling. J. Geophys. Res. Earth Surf. 115. http://dx.doi.org/10.1029/2008jf001187.
Hayakawa, Y.S., Matsukura, Y., 2010. Stability analysis of waterfall cliff face at Niagara Falls: an implication to erosional mechanism of waterfall. Eng. Geol. 116 (1–2), 178–183. http://dx.doi.org/10.1016/j.enggeo.2010.08.004.
Hodge, R.A., Hoey, T.B., Sklar, L.S., 2011. Bed load transport in bedrock rivers: the role of sediment cover in grain entrainment, translation, and deposition. J. Geophys. Res. Earth Surf. 116. http://dx.doi.org/10.1029/2011jf002032.
Holland, W.N., Pickup, G., 1976. Flume study of knickpoint development in stratified sediment. Geol. Soc. Am. Bull. 87 (1), 76–82. http://dx.doi.org/10.1130/0016-7606(1976)87<76:fsokdi>2.0.co;2.
Howard, A.D., 1994. A detachment-limited model of drainage-basin evolution. Water Resour. Res. 30 (7), 2261–2285. http://dx.doi.org/10.1029/94wr00757.
Howard, A.D., 1998. Long profile development of bedrock channels: interaction of weathering, mass wasting, bed erosion, and sediment transport. In: Tinkler, K.J., Wohl, E.E. (Eds.), Rivers Over Rock: Fluvial Processes in Bedrock Channels. Geophysical Monograph 107. American Geophysical Union, Washington, D.C., pp. 297–319.
Howard, A.D., 2007. Simulating the development of Martian highland landscapes through the interaction of impact cratering, fluvial erosion, and variable hydrologic forcing. Geomorphology 91 (3–4), 332–363. http://dx.doi.org/10.1016/j.geomorph.2007.04.017.
Howard, A.D., Kerby, G., 1983. Channel changes in badlands. Geol. Soc. Am. Bull. 94 (6), 739–752. http://dx.doi.org/10.1130/0016-7606(1983)94<739:ccib>2.0.co;2.
Howard, A.D., Dietrich, W.E., Seidl, M.A., 1994. Modeling fluvial erosion on regional to continental scales. J. Geophys. Res. Solid Earth 99 (B7), 13971–13986. http://dx.doi.org/10.1029/94jb00744.
Hsu, L., Dietrich, W.E., Sklar, L.S., 2008. Experimental study of bedrock erosion by granular flows. J. Geophys. Res. Earth Surf. 113 (F2). http://dx.doi.org/10.1029/2007jf000778.
Hu, C., Hui, Y., 1996a. Bed-load transport I: mechanical characteristics. J. Hydraul. Eng. 122, 245–254.
Hu, C., Hui, Y., 1996b. Bed-load transport II: stochastic characteristics. J. Hydraul. Eng. 122, 255–261.
Huda, S.A., Small, E.E., 2014. Modeling the effects of bed topography on fluvial bedrock erosion by saltating bed load. J. Geophys. Res. Earth Surf. http://dx.doi.org/10.1002/2013JF002872.
Iguchi, T., Sekiguchi, T., 2008. A preliminary experiment of plunge pool formation using artificial rock. University of Tsukuba Terrestrial Environment Research Center Report, 9, pp. 43–48.
Inoue, T., Izumi, N., Shimizu, Y., Parker, G., 2014. Interaction among alluvial cover, bed roughness, and incision rate in purely bedrock and alluvial-bedrock channel. J. Geophys. Res. 119, 2123–2146. http://dx.doi.org/10.1002/2014JF003133.
International Society for Rock Mechanics (ISRM), 1978. Suggested methods for determining tensile strength of rock materials. Int. J. Mech. Min. Sci. Geomech. Abstr. 21, 145–153.
Johnson, J.P.L., 2014. A surface roughness model for predicting alluvial cover and bed load transport rate in bedrock channels. J. Geophys. Res. 119, 2147–2173. http://dx.doi.org/10.1002/2013JF003000.
Johnson, J.P., Whipple, K.X., 2007. Feedbacks between erosion and sediment transport in experimental bedrock channels. Earth Surf. Process. Landf. 32 (7), 1048–1062. http://dx.doi.org/10.1002/esp.1471.
Johnson, J.P.L., Whipple, K.X., 2010. Evaluating the controls of shear stress, sediment supply, alluvial cover, and channel morphology on experimental bedrock incision rate. J. Geophys. Res. Earth Surf. 115 (F2), F02018. http://dx.doi.org/10.1029/2009JF001335.
Johnson, J.P.L., Whipple, K.X., Sklar, L.S., Hanks, T.C., 2009. Transport slopes, sediment cover, and bedrock channel incision in the Henry Mountains, Utah. J. Geophys. Res. Earth Surf. 114. http://dx.doi.org/10.1029/2007jf000862.
Johnson, J.P.L., Whipple, K.X., Sklar, L.S., 2010. Contrasting bedrock incision rates from snowmelt and flash floods in the Henry Mountains, Utah. Geol. Soc. Am. Bull. 122 (9–10), 1600–1615. http://dx.doi.org/10.1130/B30126.1.
Joseph, G.G., Hunt, M.L., 2004. Oblique particle-wall collisions in a liquid. J. Fluid Mech. 510, 71–93. http://dx.doi.org/10.1017/s002211400919x.
Joseph, G.G., Zenit, R., Hunt, M.L., Rosenwinkel, A.M., 2001. Particle-wall collisions in a viscous fluid. J. Fluid Mech. 433, 329–346.
Kirby, E., Whipple, K., 2001. Quantifying differential rock-uplift rates via stream profile analysis. Geology 29 (5), 415–418. http://dx.doi.org/10.1130/0091-7613(2001)029<0415:qdrurv>2.0.co;2.
Kirby, E., Whipple, K.X., 2012. Expression of active tectonics in erosional landscapes. J. Struct. Geol. 44, 54–75. http://dx.doi.org/10.1016/j.jsg.2012.07.009.
Kirchner, J.W., Dietrich, W.E., Iseya, F., Ikeda, H., 1990. The variability of critical shear stress, friction angle, and grain protrusion in water-worked sediments. Sedimentology 37 (4), 647–672. http://dx.doi.org/10.1111/j.1365-3091.1990.tb00627.x.
Kosmatka, S.H., Kerkhoff, B., Panarese, W.C., 2002. Design and Control of Concrete Mixtures, PCA Engineering Bulletin EB 001. Portland Cement Association, Skokie, IL.
Lague, D., Crave, A., Davy, P., 2003. Laboratory experiments simulating the geomorphic response to tectonic uplift. J. Geophys. Res. Solid Earth 108 (B1). http://dx.doi.org/10.1029/2002jb001785.
Laity, J.E., Bridges, N.T., 2009. Ventifacts on Earth and Mars: analytical, field, and laboratory studies supporting sand abrasion and windward feature development. Geomorphology 105 (3–4), 202–217. http://dx.doi.org/10.1016/j.geomorph.2008.09.014.
Lamb, M.P., Dietrich, W.E., 2009. The persistence of waterfalls in fractured rock. Geol. Soc. Am. Bull. 121 (7–8), 1123–1134. http://dx.doi.org/10.1130/b26482.1.
Lamb, M.P., Fonstad, M.A., 2010. Rapid formation of a modern bedrock canyon by a single flood event. Nat. Geosci. 3 (7), 477–481. http://dx.doi.org/10.1038/ngeo894.
Lamb, M.P., Howard, A.D., Johnson, J., Whipple, K.X., Dietrich, W.E., Perron, J.T., 2006. Can springs cut canyons into rock? J. Geophys. Res. Planets 111 (E7). http://dx.doi.org/10.1029/2005je002663.
Lamb, M.P., Howard, A.D., Dietrich, W.E., Perron, J.T., 2007. Formation of amphitheater-headed valleys by waterfall erosion after large-scale slumping on Hawai'i. Geol. Soc. Am. Bull. 119 (7–8), 805–822. http://dx.doi.org/10.1130/b25986.1.
Lamb, M.P., Dietrich, W.E., Aciego, S.M., DePaolo, D.J., Manga, M., 2008a. Formation of Box Canyon, Idaho, by megaflood: implications for seepage erosion on Earth and Mars. Science 320 (5879), 1067–1070. http://dx.doi.org/10.1126/science.1156630.
Lamb, M.P., Dietrich, W.E., Sklar, L.S., 2008b. A model for fluvial bedrock incision by impacting suspended and bed load sediment. J. Geophys. Res. Earth Surf. 113 (F3). http://dx.doi.org/10.1029/2007jf000915.
Lamb, M.P., Dietrich, W.E., Venditti, J.G., 2008c. Is the critical Shields stress for incipient sediment motion dependent on channel-bed slope? J. Geophys. Res. Earth Surf. 113 (F2), F02008. http://dx.doi.org/10.1029/2007jf000831.
Lamb, M.P., Grotzinger, J.P., Southard, J.B., Tosca, N.J., 2012. Were ripples on Mars formed by flowing brines? In: Grotzinger, J., Milliken, R. (Eds.), Sedimentary Geology on Mars. SEPM, pp. 139–150
Lamb, M.P., Mackey, B.H., Farley, K.A., 2014. Amphitheater-headed canyons formed by megaflooding at Malad Gorge, Idaho. Proc. Natl. Acad. Sci. 111 (1), 57–62. http://dx.doi.org/10.1073/pnas.1312251111.
Lang, K.A., Huntington, K.W., Montgomery, D.R., 2013. Erosion of the Tsangpo Gorge by megafloods, Eastern Himalaya. Geology 41 (9), 1003–1006. http://dx.doi.org/10.1130/g34693.1.
Lawn, B., 1993. Fracture of Brittle Solids. Cambridge University Press, New York (381 pp.).

Please cite this article as: Lamb, M.P., et al., New insights into the mechanics of fluvial bedrock erosion through flume experiments and theory, Geomorphology (2015), http://dx.doi.org/10.1016/j.geomorph.2015.03.003

Lee, H.Y., Hsu, I.S., 1994. Investigation of saltating particle motions. J. Hydraul. Eng. ASCE 120 (7), 831–845. http://dx.doi.org/10.1061/(asce)0733-9429(1994)120:7(831).

Li, X., Hunt, M.L., Colonius, T., 2012. A contact model for normal immersed collisions between a particle and a wall. J. Fluid Mech. 691, 123–145. http://dx.doi.org/10.1017/jfm.2011.461.

Limaye, A.B.S., Lamb, M.P., 2014. Numerical simulations of bedrock valley evolution by meandering rivers with variable bank material. J. Geophys. Res. Earth Surf. 119. http://dx.doi.org/10.1002/2013JF002997.

Litwin, K.L., Zygielbaum, B.R., Polito, P.J., Sklar, L.S., Collins, G.C., 2012. Influence of temperature, composition and grain size on tensile failure of water ice: implications for erosion on Titan. J. Geophys. Res. Planets 117 (E8). http://dx.doi.org/10.1029/2012JE004101.

Mackey, B.H., Scheingross, J.S., Lamb, M.P., Farley, K.A., 2014. Knickpoint formation, rapid propagation and landscape response following coastal cliff retreat at last-interglacial sea-level highstand: Kauai, Hawaii. Geol. Soc. Am. Bull. http://dx.doi.org/10.1130/B30930.1.

Malde, H.E., 1968. The catastrophic late Pleistocene Bonneville Flood in the Snake River Plain, Idaho. USGS Prof. Pap. 596, 1–52.

Manga, M., Kirchner, J.W., 2000. Stress partitioning in streams by large woody debris. Water Resour. Res. 36 (8), 2373–2379. http://dx.doi.org/10.1029/2000wr900153.

Manso, P.A., Bollaert, E.F.R., Schleiss, A.J., 2009. Influence of plunge pool geometry on high-velocity jet impact pressures and pressure propagation inside fissured rock media. J. Hydraul. Eng. ASCE 135 (10), 783–792. http://dx.doi.org/10.1061/(asce)hy.1943-7900.0000090.

Martel, S.J., 2006. Effect of topographic curvature on near-surface stresses and application to sheeting joints. Geophys. Res. Lett. 33 (1). http://dx.doi.org/10.1029/2005gl024710.

McLean, S.R., 1991. Depth-integrated suspended-load calculations. J. Hydraul. Eng. ASCE 117 (11), 1440–1458. http://dx.doi.org/10.1061/(asce)0733-9429(1991)117:11(1440).

McLean, S.R., 1992. On the calculation of suspended-load for noncohesive sediments. J. Geophys. Res. Oceans 97 (C4), 5759–5770. http://dx.doi.org/10.1029/91jc02933.

Melville, B., van Ballegooy, R., van Ballegooy, S., 2006. Flow-induced failure of cable-tied blocks. J. Hydraul. Eng. ASCE 132 (3), 324–327. http://dx.doi.org/10.1061/(asce)0733-9429(2006)132:3(324).

Miller, J.R., 1991. The influence of bedrock geology on knickpoint development and channel-bed degradation along downcutting streams in south-central Indiana. J. Geol. 99 (4), 591–605.

Miller, D.J., Dunne, T., 1996. Topographic perturbations of regional stresses and consequent bedrock fracturing. J. Geophys. Res. Solid Earth 101 (B11), 25523–25536. http://dx.doi.org/10.1029/96jb02531.

Nelson, P.K., 2003. Handbook of nondestructive and innovative testing equipment for concrete. Final Report. Federal Highway Administration, Washington, D.C.

Nelson, P.A., Seminara, G., 2011. Modeling the evolution of bedrock channel shape with erosion from saltating bed load. Geophys. Res. Lett. 38 (17), L17406. http://dx.doi.org/10.1029/2011GL048628.

Nelson, P.A., Seminara, G., 2012. A theoretical framework for the morphodynamics of bedrock channels. Geophys. Res. Lett. 39 (6), L06408. http://dx.doi.org/10.1029/2011GL050806.

Nino, Y., Garcia, M., Ayala, L., 1994. Gravel saltation: 1 experiments. Water Resour. Res. 30 (6), 1907–1914. http://dx.doi.org/10.1029/94wr00533.

Nino, Y., Lopez, F., Garcia, M., 2003. Threshold for particle entrainment into suspension. Sedimentology 50 (2), 247–263. http://dx.doi.org/10.1046/j.1365-3091.2003.00551.x.

Nittrouer, J.A., Mohrig, D., Allison, M.A., Peyret, A.-P.B., 2011. The lowermost Mississippi River: a mixed bedrock-alluvial channel. Sedimentology 58 (7), 1914–1934. http://dx.doi.org/10.1111/j.1365-3091.2011.01245.x.

Ouimet, W.B., Whipple, K.X., Granger, D.E., 2009. Beyond threshold hillslopes: channel adjustment to base-level fall in tectonically active mountain ranges. Geology 37 (7), 579–582. http://dx.doi.org/10.1130/g30013a.1.

Paola, C., Straub, K., Mohrig, D., Reinhardt, L., 2009. The "unreasonable effectiveness" of stratigraphic and geomorphic experiments. Earth Sci. Rev. 97 (1–4), 1–43. http://dx.doi.org/10.1016/j.earscirev.2009.05.003.

Parker, G., 1991. Selective sorting and abrasion of river gravel: II applications. J. Hydraul. Eng. 117 (2), 150–171.

Parker, G., Izumi, N., 2000. Purely erosional cyclic and solitary steps created by flow over a cohesive bed. J. Fluid Mech. 419, 203–238. http://dx.doi.org/10.1017/s0022112000001403.

Parker, G., Wilcock, P.R., Paola, C., Dietrich, W.E., Pitlick, J., 2007. Physical basis for quasi-universal relations describing bankfull hydraulic geometry of single-thread gravel bed rivers. J. Geophys. Res. Earth Surf. 112. http://dx.doi.org/10.1029/2006jf000549.

Peakall, J., Ashworth, P., Best, J.L., 1996. Physical modelling in fluvial geomorphology: principles, applications and unresolved issues. In: Rhoads, L.B., Thorn, E.C. (Eds.), The Scientific Nature of Geomorphology. Wiley & Sons, Chichester, pp. 221–253.

Pederson, J.L., Anders, M.D., Rittenhour, T.M., Sharp, W.D., Gosse, J.C., Karlstrom, K.E., 2006. Using fill terraces to understand incision rates and evolution of the Colorado River in eastern Grand Canyon, Arizona. J. Geophys. Res. Earth Surf. 111 (F2). http://dx.doi.org/10.1029/2004jf000201.

Perron, J.T., Lamb, M.P., Koven, C.D., Fung, I.Y., Yager, E., Adamkovics, M., 2006. Valley formation and methane precipitation rates on Titan. J. Geophys. Res. Planets 111 (E11). http://dx.doi.org/10.1029/2005je002602.

Perron, J.T., Dietrich, W.E., Kirchner, J.W., 2008. Controls on the spacing of first-order valleys. J. Geophys. Res. Earth Surf. 113 (F4). http://dx.doi.org/10.1029/2007jf000977.

Prancevic, J.P., Lamb, M.P., Fuller, B.M., 2014. Incipient sediment motion across the river to debris-flow transition. Geology 42 (3), 191–194. http://dx.doi.org/10.1130/g34927.1.

Reinius, E., 1986. Rock erosion. Water Power Dam Constr. 38 (6), 43–48.

Reneau, S.L., 2000. Stream incision and terrace development in Frijoles Canyon, Bandelier National Monument, New Mexico, and the influence of lithology and climate. Geomorphology 32 (1), 171–193.

Reusser, L.J., Bierman, P.R., Pavich, M.J., Zen, E.A., Larsen, J., Finkel, R., 2004. Rapid Late Pleistocene incision of Atlantic passive-margin river gorges. Science 305 (5683), 499–502.

Richardson, K., Carling, P.A., 2006. The hydraulics of a straight bedrock channel: insights from solute dispersion studies. Geomorphology 82 (1), 98–125.

Roberts, G.G., White, N.J., Martin-Brandis, G.L., Crosby, A.G., 2012. An uplift history of the Colorado Plateau and its surroundings from inverse modeling of longitudinal river profiles. Tectonics 31. http://dx.doi.org/10.1029/2012tc003107.

Robinson, K.M., Hanson, G.J., Cook, K.R., Kadavy, K.C., 2001. Erosion of fractured materials. Trans. ASAE 44 (4), 819–823.

Rouse, H.R., 1936. Discharge characteristics of the free overfall. Civ. Eng. 7, 518.

Rouse, H.R., 1937. Modern conceptions of the mechanics of turbulence. Trans. Am. Soc. Civ. Eng. 102 (1), 463–543.

Scheingross, J.S., Winchell, E.W., Lamb, M.P., Dietrich, W.E., 2013. Influence of bed patchiness, slope, grain hiding, and form drag on gravel mobilization in very steep streams. J. Geophys. Res. Earth Surf. 118 (2), 982–1001. http://dx.doi.org/10.1002/jgrf.20067.

Scheingross, J.S., Brun, F., Lo, D.Y., Omerdin, K., Lamb, M.P., 2014. Experimental evidence for fluvial bedrock incision by suspended and bedload sediment. Geology 42 (6). http://dx.doi.org/10.1130/G35432.1.

Schlichting, H., 1979. Boundary-layer Theory. McGraw-Hill.

Schmeeckle, M.W., Nelson, J.M., Pitlick, J., Bennett, J.P., 2001. Interparticle collision of natural sediment grains in water. Water Resour. Res. 37 (9), 2377–2391. http://dx.doi.org/10.1029/2001wr000531.

Schmeeckle, M.W., Nelson, J.M., Shreve, R.L., 2007. Forces on stationary particles in near-bed turbulent flows. J. Geophys. Res. Earth Surf. 112 (F2). http://dx.doi.org/10.1029/2006jf000536.

Schumm, S.A., Mosley, M.P., Weaver, W., 1987. Experimental Fluvial Geomorphology. John Wiley & Sons, New York (413 pp.).

Selby, M.J., 1993. Hillslope Materials and Processes. Oxford University Press, Oxford (451 pp.).

Shaw, J.B., Mohrig, D., Whitman, S.K., 2013. The morphology and evolution of channels on the Wax Lake Delta, Louisiana, USA. J. Geophys. Res. Earth Surf. 118 (3), 1562–1584. http://dx.doi.org/10.1002/jgrf.20123.

Shepherd, R.G., Schumm, S.A., 1974. Experimental study of river incision. Geol. Soc. Am. Bull. 85 (2), 257–268. http://dx.doi.org/10.1130/0016-7606(1974)85<257:Esori>2.0.Co;2.

Shields, A., 1936. Application of similarity principles and turbulence research to bed-load movement. U.S. Dept of Agriculture Soil Conservation Service Cooperative Laboratory. Hydrodynamics Laboratory Publication 167. California Institute of Technology, Pasadena, CA.

Sklar, L.S., Dietrich, W.E., 1998. River longitudinal profiles and bedrock incision models: stream power and the influence of sediment supply. In: Tinkler, K.J., Wohl, E.E. (Eds.), Rivers Over Rock: Fluvial Processes in Bedrock Channels. Geophysical Monograph 107. American Geophysical Union, Washington, D.C., pp. 237–260.

Sklar, L.S., Dietrich, W.E., 2001. Sediment and rock strength controls on river incision into bedrock. Geology 29 (12), 1087–1090. http://dx.doi.org/10.1130/0091-7613(2001)029<1087:sarsco>2.0.co;2.

Sklar, L.S., Dietrich, W.E., 2004. A mechanistic model for river incision into bedrock by saltating bed load. Water Resour. Res. 40 (6). http://dx.doi.org/10.1029/2003wr002496.

Sklar, L.S., Dietrich, W.E., 2006. The role of sediment in controlling steady-state bedrock channel slope: implications of the saltation–abrasion incision model. Geomorphology 82 (1–2), 58–83. http://dx.doi.org/10.1016/j.geomorph.2005.08.019.

Sklar, L.S., Dietrich, W.E., 2008. Implications of the saltation–abrasion bedrock incision model for steady-state river longitudinal profile relief and concavity. Earth Surf. Process. Landf. 33 (7), 1129–1151. http://dx.doi.org/10.1002/esp.1689.

Sklar, L.S., Dietrich, W.E., 2012. Correction to "A mechanistic model for river incision into bedrock by saltating bed load". Water Resour. Res. 48. http://dx.doi.org/10.1029/2012wr012267.

Sklar, L.S., Collins, G.C., Litwin, K.L., Polito, P.J., Zygielbaum, B.R., 2012. Erodibility of Titan ice bedrock constrained by laboratory measurements of ice strength and erosion by sediment impacts. Eos Trans. AGU 93 (52) (Fall Suppl., Abstract EP44A-06).

Small, E.E., Hancock, G., Wobus, C.W., 2012. Variations in rock erodibility across bedrock-floored stream channels. Eos Trans. AGU 93 (52) (Fall Suppl., Abstract EP13A-0815).

Smith, C.E., 1998. Modeling high sinuosity meanders in a small flume. Geomorphology 25 (1), 19–30.

Stein, O.R., Julien, P.Y., 1994. Sediment concentration below free overfall. J. Hydraul. Eng. ASCE 120 (9), 1043–1059. http://dx.doi.org/10.1061/(asce)0733-9429(1994)120:9(1043).

Stein, O.R., LaTray, D.A., 2002. Experiments and modeling of head cut migration in stratified soils. Water Resour. Res. 38 (12). http://dx.doi.org/10.1029/2001wr001166.

Stein, O.R., Alonso, C.V., Julien, P.Y., 1993. Mechanics of jet scour downstream of a headcut. J. Hydraul. Res. 31 (6), 723–738.

Stock, J.D., Montgomery, D.R., 1999. Geologic constraints on bedrock river incision using the stream power law. J. Geophys. Res. Solid Earth 104 (B3), 4983–4993. http://dx.doi.org/10.1029/98jb02139.

Stock, J.D., Montgomery, D.R., Collins, B.D., Dietrich, W.E., Sklar, L., 2005. Field measurements of incision rates following bedrock exposure: implications for process controls on the long profiles of valleys cut by rivers and debris flows. Geol. Soc. Am. Bull. 117 (1–2), 174–194. http://dx.doi.org/10.1130/b25560.1.

Taki, K., Parker, G., 2005. Transportational cyclic steps created by flow over an erodible bed. Part 1. Experiments. J. Hydraul. Res. 43 (5), 488–501.

Thompson, D., Wohl, E., 1998. Flume experimentation and simulation of bedrock channel processes. In: Tinkler, K.J., Wohl, E.E. (Eds.), Rivers Over Rock: Fluvial Processes in Bedrock Channels. Geophysical Monograph 107. American Geophysical Union, Washington, D.C.

Tinkler, K.J., Wohl, E., 1998. A primer on bedrock channels. In: Tinkler, K.J., Wohl, E.E. (Eds.), Rivers Over Rock: Fluvial Processes in Bedrock Channels. Geophysical Monograph Series 107. American Geophysical Union, Washington DC, pp. 1–18.

Please cite this article as: Lamb, M.P., et al., New insights into the mechanics of fluvial bedrock erosion through flume experiments and theory, Geomorphology (2015), http://dx.doi.org/10.1016/j.geomorph.2015.03.003

Tsujimoto, T., 1999. Sediment transport processes and channel incision: mixed size sediment transport, degradation and armoring. In: Darby, S.E., Simon, A. (Eds.), Incised River Channels. John Wiley, Hoboken, NJ, pp. 37–67.
U.S. Bureau of Reclamation (USBR), 2007. Uplift and crack flow resulting from high velocity discharges over open offset joints. Report DSO-07-07. United States Bureau of Reclamation, Denver.
Weissel, J.K., Seidl, M.A., 1997. Influence of rock strength properties on escarpment retreat across passive continental margins. Geology 25 (7), 631–634. http://dx.doi.org/10.1130/0091-7613(1997)025<0631:iorspo>2.3.co;2.
Wells, R.R., Bennett, S.J., Alonso, C.V., 2010. Modulation of headcut soil erosion in rills due to upstream sediment loads. Water Resour. Res. 46, W12531. http://dx.doi.org/10.1029/2010WR009433.
Whipple, K.X., 2004. Bedrock rivers and the geomorphology of active orogens. Annu. Rev. Earth Planet. Sci. 32, 151–185. http://dx.doi.org/10.1146/annurev.earth.32.101802.120356.
Whipple, K.X., Hancock, G.S., Anderson, R.S., 2000. River incision into bedrock: mechanics and relative efficacy of plucking, abrasion, and cavitation. Geol. Soc. Am. Bull. 112 (3), 490–503. http://dx.doi.org/10.1130/0016-7606(2000)112<0490:riibma>2.3.co;2.
Whipple, K.X., DiBiase, R.A., Crosby, B.T., 2013. Bedrock rivers. In: Shroder Jr., J., Wohl, E.E. (Eds.), Treatise on Geomorphology. Academic Press, San Diego.
Wiberg, P.L., Smith, J.D., 1987. Calculations of the critical shear-stress for motion of uniform and heterogeneous sediments. Water Resour. Res. 23 (8), 1471–1480. http://dx.doi.org/10.1029/WR023i008p01471.
Wilcock, P.R., 1993. Critical shear-stress of natural sediments. J. Hydraul. Eng. ASCE 119 (4), 491–505.
Willett, S.D., 1999. Orogeny and orography: the effects of erosion on the structure of mountain belts. J. Geophys. Res. Solid Earth 104 (B12), 28957–28981. http://dx.doi.org/10.1029/1999jb900248.
Wilson, A., Lavé, J., 2014. Convergent evolution of abrading flow obstacles: insights from analogue modelling of fluvial bedrock abrasion by coarse bedload. Geomorphology 208, 207–224. http://dx.doi.org/10.1016/j.geomorph.2013.11.024.
Wilson, A., Hovius, N., Turowski, J.M., 2013. Upstream-facing convex surfaces: bedrock bedforms produced by fluvial bedload abrasion. Geomorphology 180, 187–204. http://dx.doi.org/10.1016/j.geomorph.2012.10.010.
Wobus, C.W., Crosby, B.T., Whipple, K.X., 2006. Hanging valleys in fluvial systems: controls on occurrence and implications for landscape evolution. J. Geophys. Res. Earth Surf. 111 (F2). http://dx.doi.org/10.1029/2005jf000406.
Wohl, E., Ikeda, H., 1997. Experimental simulation of channel incision into a cohesive substrate at varying gradients. Geology 25 (4), 295–298. http://dx.doi.org/10.1130/0091-7613(1997)025<0295:esocii>2.3.co;2.
Yager, E.M., Kirchner, J.W., Dietrich, W.E., 2007. Calculating bed load transport in steep boulder bed channels. Water Resour. Res. 43 (7). http://dx.doi.org/10.1029/2006wr005432.
Yalin, M.S., 1977. Mechanics of Sediment Transport. Pergamon Press, Oxford.
Yokokawa, M., Kyogoku, A., Kotera, A., Izumi, N., 2013. Cyclic steps incised on experimental bedrock. Eos Trans. AGU 94 (52) (Fall Suppl., Abstract EP24B-06).
Young, R.W., 1983. The tempo of geomorphological change: evidence from southeastern Australia. J. Geol. 91 (2), 221–230.
Young, R., McDougall, I., 1993. Long-term landscape evolution: Early Miocene and modern rivers in southern New South Wales, Australia. J. Geol. 101 (1), 35–49.

Please cite this article as: Lamb, M.P., et al., New insights into the mechanics of fluvial bedrock erosion through flume experiments and theory, Geomorphology (2015), http://dx.doi.org/10.1016/j.geomorph.2015.03.003